

Second-Order Sensitivity Analysis of Uncollided Particle Contributions to Radiation Detector Responses

Dan G. Cacuci & Jeffrey A. Favorite

To cite this article: Dan G. Cacuci & Jeffrey A. Favorite (2018) Second-Order Sensitivity Analysis of Uncollided Particle Contributions to Radiation Detector Responses, Nuclear Science and Engineering, 190:2, 105-133, DOI: [10.1080/00295639.2018.1426899](https://doi.org/10.1080/00295639.2018.1426899)

To link to this article: <https://doi.org/10.1080/00295639.2018.1426899>



Published with license by Taylor & Francis. © Dan G. Cacuci and Jeffrey A. Favorite.



Published online: 06 Apr 2018.



Submit your article to this journal [↗](#)



Article views: 574



View related articles [↗](#)



View Crossmark data [↗](#)



Citing articles: 1 View citing articles [↗](#)



Second-Order Sensitivity Analysis of Uncollided Particle Contributions to Radiation Detector Responses

Dan G. Cacuci^{a*} and Jeffrey A. Favorite^b

^aUniversity of South Carolina, Columbia, South Carolina 29208

^bLos Alamos National Laboratory, Computational Physics (X-CP) Division, MS F663, Los Alamos, New Mexico 87545

Received October 10, 2017

Accepted for Publication January 9, 2018

Abstract — This work presents an application of Cacuci's Second-Order Adjoint Sensitivity Analysis Methodology (2nd-ASAM) to the simplified Boltzmann equation that models the transport of uncollided particles through a medium to compute efficiently and exactly all of the first- and second-order derivatives (sensitivities) of a detector's response with respect to the system's isotopic number densities, microscopic cross sections, source emission rates, and detector response function. The off-the-shelf PARTISN multigroup discrete ordinates code is employed to solve the equations underlying the 2nd-ASAM. The accuracy of the results produced using PARTISN is verified by using the results of three test configurations: (1) a homogeneous sphere, for which the response is the exactly known total uncollided leakage, (2) a multiregion two-dimensional (r - z) cylinder, and (3) a two-region sphere for which the response is a reaction rate. For the homogeneous sphere, results for the total leakage as well as for the respective first- and second-order sensitivities are in excellent agreement with the exact benchmark values. For the nonanalytic problems, the results obtained by applying the 2nd-ASAM to compute sensitivities are in excellent agreement with central-difference estimates. The efficiency of the 2nd-ASAM is underscored by the fact that, for the cylinder, only 12 adjoint PARTISN computations were required by the 2nd-ASAM to compute all of the benchmark's 18 first-order sensitivities and 224 second-order sensitivities, in contrast to the 877 PARTISN calculations needed to compute the respective sensitivities using central finite differences, and this number does not include the additional calculations that were required to find appropriate values of the perturbations to use for the central differences.

Keywords — Second-order adjoint sensitivity analysis, particle and radiation transport, response variance and skewness.

Note — Some figures may be in color only in the electronic version.

I. INTRODUCTION

This work presents the application of the Second-Order Adjoint Sensitivity Analysis Methodology (2nd-ASAM),

developed by Cacuci,^{1,2} to the simplified Boltzmann equation describing the transport of uncollided neutrons or gamma rays in a medium to compute all of the first- and second-order derivatives (also known as *sensitivities*) of a detector response with respect to the system's isotopic number densities, microscopic cross sections, source emission rates, and detector response parameters. The 2nd-ASAM is the most efficient methodology for computing exactly and efficiently the first-order sensitivities (using a single adjoint computation) and the second-order sensitivities (using at most as many large-scale computations as there are parameters in the system under investigation), since the number of large-scale computations

*E-mail: cacuci@cec.sc.edu

This is an Open Access article distributed under the terms of the Creative Commons Attribution-NonCommercial-NoDerivatives License (<http://creativecommons.org/licenses/by-nc-nd/4.0/>), which permits non-commercial re-use, distribution, and reproduction in any medium, provided the original work is properly cited, and is not altered, transformed, or built upon in any way.

using the 2nd-ASAM increases only linearly with the number of system parameters. In contradistinction, the number of large-scale computations needed by all of the other methods currently used for computing higher-order response sensitivities increase exponentially with the number of system parameters.

The second-order sensitivities contribute the leading correction terms to the response's expected value, causing it to differ from the response's computed value.³⁻⁵ The second-order sensitivities also contribute the leading terms to the response's third-order moments, which determine the *skewness* of a response. Events occurring in a response's long and/or short tails, which are characteristic of rare but decisive events (e.g., major accidents, catastrophes), would likely be missed if the second-order sensitivities were ignored.

This paper is organized as follows. Section II presents the Boltzmann transport equation describing the transport of uncollided particles within a finite medium and defining the physical system's parameters and responses. Section III presents the construction of the First-Level Adjoint Sensitivity System (1st-LASS) for the transport equation. The 1st-LASS is used for the efficient computation of the first-order response sensitivities to variations in model parameters, and it serves as the basis for the construction of the Second-Level Adjoint Sensitivity System (2nd-LASS). The actual construction of the 2nd-LASS for the transport equation is presented in Sec. IV, which also presents the specific expressions for computing exactly and efficiently all of the second-order response sensitivities to variations in model parameters. Sections V, VI, and VII present numerical results for test problems in spherical and cylindrical geometries. The sensitivities of the total uncollided leakage for the homogeneous sphere (Sec. V) can be computed analytically,^{6,7} thus serving as a stringent verification of the numerical accuracy produced by the off-the-shelf PARTISN multigroup discrete ordinates code,⁸ which has been used to solve the equations underlying the 2nd-ASAM. Section VIII summarizes and concludes this work.

II. THE FORWARD BOLTZMANN EQUATION FOR UNCOLLIDED PARTICLES

The angular flux $\varphi(\mathbf{r}, \boldsymbol{\Omega})$ of uncollided neutrons or gamma rays in a finite medium placed in vacuum satisfies the transport (Boltzmann) equation with no scattering source⁶:

$$\boldsymbol{\Omega} \cdot \nabla \varphi(\mathbf{r}, \boldsymbol{\Omega}) + \Sigma_t(\mathbf{r}) \varphi(\mathbf{r}, \boldsymbol{\Omega}) = q(\mathbf{r}) \quad (1)$$

subject to the vacuum boundary condition that specifies there is no incoming flux of particles:

$$\varphi(\mathbf{r}_s, \boldsymbol{\Omega}) = 0, \mathbf{r}_s \in \partial V, \boldsymbol{\Omega} \cdot \mathbf{n} < 0 \quad (2)$$

where

$\boldsymbol{\Omega}$ = unit vector in the direction of the particle's (neutron or photon) motion

\mathbf{r} = particle's position

$\Sigma_t(\mathbf{r})$ = total interaction cross section

$q(\mathbf{r})$ = particle source density (particles/cubic centimeters/seconds), assumed to be isotropic

V = body's volume

\mathbf{n} = unit outward normal vector at any point $\mathbf{r}_s \in \partial V$ on the body's outer surface ∂V .

The quantity of interest is a detector response, denoted as $R(\varphi, \boldsymbol{\alpha})$, of the form

$$R(\varphi, \boldsymbol{\alpha}) = \int dV \int_{4\pi} d\boldsymbol{\Omega} \Sigma_d(\mathbf{r}, \boldsymbol{\Omega}) \varphi(\mathbf{r}, \boldsymbol{\Omega}) \quad (3)$$

where $\Sigma_d(\mathbf{r}, \boldsymbol{\Omega})$ models the interaction of the detector with the incident particles. The detector responses of particular interest are: (1) the scalar flux at a point, in which case the detector-interaction function has the form

$$\Sigma_d(\mathbf{r}, \boldsymbol{\Omega}) = \delta(\mathbf{r} - \mathbf{r}_d) \quad (4)$$

where \mathbf{r}_d represents the detector's location, and (2) the partial current density at a point, in which case the detector-interaction function has the form

$$\Sigma_d(\mathbf{r}, \boldsymbol{\Omega}) = \boldsymbol{\Omega} \cdot \mathbf{n} \delta(\mathbf{r} - \mathbf{r}_d) \quad (5)$$

where \mathbf{n} is a unit vector normal to the unit area at \mathbf{r}_d through which the partial current density is to be calculated. Equations (4) and (5) can easily be modified to compute the flux or partial current density over an entire surface.

The quantities $\Sigma_t(\mathbf{r})$, $q(\mathbf{r})$, and $\Sigma_d(\mathbf{r}, \boldsymbol{\Omega})$ depend not only on the spatial variable \mathbf{r} but also on model parameters such as atomic number densities, microscopic cross sections, and weighting functions. Therefore, it is convenient to denote generically the model's parameters as α_j , and to consider that these model parameters are ordered as the components of a (column) vector of model parameters denoted as $\boldsymbol{\alpha}$ and defined as

$$\boldsymbol{\alpha} \triangleq [\alpha_1, \dots, \alpha_{N_a}]^T \quad (6)$$

The model parameters are not perfectly well known; it is considered that their nominal values, which will be denoted as $\boldsymbol{\alpha}^0 \triangleq [\alpha_1^0, \dots, \alpha_{N_\alpha}^0]^\dagger$, and their corresponding standard deviations, which will be denoted as $\boldsymbol{\sigma} \triangleq [\sigma_1, \dots, \sigma_{N_\alpha}]^\dagger$, are available. Throughout this paper, the dagger (\dagger) is used to denote transposition and the superscript zero is used to denote nominal values.

Although the medium in which the neutrons and/or gamma rays propagate is heterogeneous, the material properties $\Sigma_t(\mathbf{r})$, $q(\mathbf{r})$, and $\Sigma_d(\mathbf{r}, \boldsymbol{\Omega})$ are often piecewise constant within the various material regions which make up the respective medium. Usually, the heterogeneous medium under consideration comprises N_m layers of materials having piecewise constant properties within each layer. In such cases, the quantities $\Sigma_t(\mathbf{r})$, $q(\mathbf{r})$, and $\Sigma_d(\mathbf{r}, \boldsymbol{\Omega})$ can be represented as follows:

$$\Sigma_t(\mathbf{r}) = \sum_{j=1}^{N_m} C_j(\boldsymbol{\alpha}) f_j(\mathbf{r}) \quad (7)$$

$$q(\mathbf{r}) = \sum_{j=1}^{N_m} Q_j(\boldsymbol{\alpha}) g_j(\mathbf{r}) \quad (8)$$

and

$$f_j(\mathbf{r}) = g_j(\mathbf{r}) = H(\mathbf{r} - \mathbf{r}_j) - H(\mathbf{r} - \mathbf{r}_{j+1}), \quad (9)$$

$j = 1, \dots, N_m$,

where

- $C_j(\boldsymbol{\alpha}), Q_j(\boldsymbol{\alpha})$ = parameter-dependent coefficients
- $f_j(\mathbf{r}), g_j(\mathbf{r})$ = corresponding piecewise spatial variation of the cross sections and sources, respectively
- $H(\mathbf{r} - \mathbf{r}_j)$ = customary Heaviside unit-functional
- \mathbf{r}_j = j 'th-material interface, with \mathbf{r}_1 denoting the coordinate(s) of the innermost material boundary.

When the detector consists of N_d layers of materials having piecewise constant properties, represented by interaction coefficients $\mu_k(\boldsymbol{\alpha})$ within each layer, the effective detector cross section may be represented in a form similar to Eq. (7), namely

$$\Sigma_d(\mathbf{r}, \boldsymbol{\Omega}) = \sum_{k=1}^{N_d} \mu_k(\boldsymbol{\alpha}) h_k(\mathbf{r}, \boldsymbol{\Omega}) \quad (10)$$

In this paper, the space-dependent functions $f_j(\mathbf{r})$, $g_j(\mathbf{r})$, and $h_k(\mathbf{r}, \boldsymbol{\Omega})$, which describe internal boundaries, will be considered to be perfectly well known. Situations with uncertain internal and/or external boundaries will be considered in subsequent work. Linear and/or nonlinear spatial dependence of material properties can also be accommodated by suitable definitions of the functions $f_j(\mathbf{r})$, $g_j(\mathbf{r})$, and $h_k(\mathbf{r}, \boldsymbol{\Omega})$.

III. FIRST-LEVEL FORWARD AND ADJOINT SENSITIVITY SYSTEMS FOR COMPUTING FIRST-ORDER RESPONSE SENSITIVITIES TO VARIATIONS IN MODEL PARAMETERS

The nominal value of the angular flux $\varphi^0(\mathbf{r}, \boldsymbol{\Omega})$ is obtained by solving Eqs. (1) and (2) using the nominal parameter values, i.e., $\varphi^0(\mathbf{r}, \boldsymbol{\Omega})$ is the solution of

$$\boldsymbol{\Omega} \cdot \nabla \varphi^0(\mathbf{r}, \boldsymbol{\Omega}) + \Sigma_t^0(\mathbf{r}) \varphi^0(\mathbf{r}, \boldsymbol{\Omega}) = q^0(\mathbf{r}) \quad (11)$$

subject to the vacuum boundary condition which specifies that there is no incoming flux of particles:

$$\varphi^0(\mathbf{r}_s, \boldsymbol{\Omega}) = 0, \mathbf{r}_s \in \partial V, \boldsymbol{\Omega} \cdot \mathbf{n} < 0 \quad (12)$$

The nominal value of the detector response R^0 is obtained by evaluating Eq. (3) at the nominal flux and parameter values:

$$R^0 \triangleq R(\varphi^0, \boldsymbol{\alpha}^0) = \int dV \int_{4\pi} d\boldsymbol{\Omega} \Sigma_d^0(\mathbf{r}, \boldsymbol{\Omega}) \varphi^0(\mathbf{r}, \boldsymbol{\Omega}) \quad (13)$$

The total sensitivity $\delta R(\varphi^0, \boldsymbol{\alpha}^0; \delta\varphi, \delta\boldsymbol{\alpha})$ of the detector response defined in Eq. (3) to variations $\delta\boldsymbol{\alpha} \triangleq [\delta\alpha_1, \dots, \delta\alpha_{N_\alpha}]^\dagger$ in the model parameters, around the nominal values $\boldsymbol{\alpha}^0$, is obtained by computing the Gateaux (G-) differential of Eq. (3) at the nominal parameter and flux values, which is obtained from its definition, as follows:

$$\begin{aligned} \delta R(\varphi^0, \mathbf{a}^0; \delta\varphi, \delta\mathbf{a}) &\triangleq \frac{d}{d\varepsilon} \left\{ \int dV \int_{4\pi} d\Omega [\Sigma_d^0(\mathbf{r}, \Omega) \right. \\ &\quad \left. + \varepsilon \delta \Sigma_d(\mathbf{r}, \Omega)] [\varphi^0(\mathbf{r}, \Omega) + \varepsilon \delta\varphi(\mathbf{r}, \Omega)] \right\}_{\varepsilon=0} \\ &= \{ \delta R(\varphi^0, \mathbf{a}^0; \delta\mathbf{a}) \}_{dir} + \{ \delta R(\varphi^0, \mathbf{a}^0; \delta\varphi, \delta\mathbf{a}) \}_{ind}, \end{aligned} \quad (14)$$

where the *direct-effect* term is defined as

$$\{ \delta R(\varphi, \mathbf{a}; \delta\mathbf{a}) \}_{dir} \triangleq \int dV \int_{4\pi} \delta \Sigma_d(\mathbf{r}, \Omega) \varphi(\mathbf{r}, \Omega) d\Omega, \quad (15)$$

and where the *indirect-effect* term is defined as

$$\{ \delta R(\varphi, \mathbf{a}; \delta\varphi, \delta\mathbf{a}) \}_{ind} \triangleq \int dV \int_{4\pi} d\Omega \Sigma_d(\mathbf{r}, \Omega) \delta\varphi(\mathbf{r}, \Omega). \quad (16)$$

The variation $\delta\varphi(\mathbf{r}, \Omega)$ that appears in Eq. (16) is the solution^{3,5} of the First-Level Forward Sensitivity System (1st-LFSS), which is derived by G-differentiating Eqs. (1) and (2) to obtain

$$\begin{aligned} \mathbf{\Omega} \cdot \nabla \delta\varphi(\mathbf{r}, \Omega) + \Sigma_t^0(\mathbf{r}) \delta\varphi(\mathbf{r}, \Omega) \\ = \delta q(\mathbf{r}) - \delta \Sigma_t(\mathbf{r}) \varphi^0(\mathbf{r}, \Omega) \end{aligned} \quad (17)$$

and

$$\delta\varphi(\mathbf{r}_s, \Omega) = 0, \mathbf{r}_s \in \partial V, \mathbf{\Omega} \cdot \mathbf{n} < 0. \quad (18)$$

In view of Eqs. (7) through (10), the variations $\delta \Sigma_t(\mathbf{r})$, $\delta q(\mathbf{r})$, and $\delta \Sigma_d(\mathbf{r}, \Omega)$ which appear in Eqs. (15) and (17) are defined as follows:

$$\delta \Sigma_t(\mathbf{r}) = \sum_{j=1}^{N_m} \left[\sum_{k=1}^{N_a} \frac{\partial C_j(\mathbf{a})}{\partial \mathbf{a}_k} \delta \mathbf{a}_k \right] f_j(\mathbf{r}), \quad (19)$$

$$\delta q(\mathbf{r}) = \sum_{j=1}^{N_m} \left[\sum_{k=1}^{N_a} \frac{\partial Q_j(\mathbf{a})}{\partial \mathbf{a}_k} \delta \mathbf{a}_k \right] g_j(\mathbf{r}), \quad (20)$$

and

$$\delta \Sigma_d(\mathbf{r}, \Omega) = \sum_{j=1}^{N_d} \left[\sum_{k=1}^{N_a} \frac{\partial \mu_j(\mathbf{a})}{\partial \mathbf{a}_k} \delta \mathbf{a}_k \right] h_j(\mathbf{r}, \Omega). \quad (21)$$

The indirect-effect term defined in Eq. (16) can be computed only after solving the 1st-LFSS, which is computationally

expensive, since the 1st-LFSS would need to be solved anew for every variation in the model parameters. As is well known, the computationally expensive evaluation of the indirect-effect term by using Eq. (16) can be avoided by expressing this indirect-effect term in terms of the solution of the 1st-LASS,^{1,2} which is constructed by implementing the following sequence of steps:

1. Define the inner product $\langle u(\mathbf{r}, \Omega), w(\mathbf{r}, \Omega) \rangle$ of two functions $u(\mathbf{r}, \Omega) \in L_2(V \times \Omega)$ and $w(\mathbf{r}, \Omega) \in L_2(V \times \Omega)$ in the Hilbert space $L_2(V \times \Omega)$ of square-integrable functions, as follows:

$$\langle u(\mathbf{r}, \Omega), w(\mathbf{r}, \Omega) \rangle \triangleq \int dV \int_{4\pi} d\Omega u(\mathbf{r}, \Omega) w(\mathbf{r}, \Omega). \quad (22)$$

2. Form the inner product of Eq. (17) with a yet undefined function $\psi^{(1)}(\mathbf{r}, \Omega)$ to obtain

$$\begin{aligned} \langle \psi^{(1)}(\mathbf{r}, \Omega), \mathbf{\Omega} \cdot \nabla \delta\varphi(\mathbf{r}, \Omega) + \Sigma_t^0(\mathbf{r}) \delta\varphi(\mathbf{r}, \Omega) \rangle \\ = \langle \psi^{(1)}(\mathbf{r}, \Omega), \delta q(\mathbf{r}) - \delta \Sigma_t(\mathbf{r}) \varphi^0(\mathbf{r}, \Omega) \rangle. \end{aligned} \quad (23)$$

3. For a linear operator $L^{(1)}$ use the Hilbert space $L_2(V \times \Omega)$ with the inner product defined in Eq. (22) to define the formal adjoint operator, denoted as $A^{(1)}$, of $L^{(1)}$, through the following relationship:

$$\langle \psi^{(1)}, L^{(1)} \delta\varphi \rangle = \langle \delta\varphi, A^{(1)} \psi^{(1)} \rangle + P^{(1)}(\delta\varphi, \psi^{(1)}), \quad (24)$$

where

$$L^{(1)} \delta\varphi \triangleq \mathbf{\Omega} \cdot \nabla \delta\varphi(\mathbf{r}, \Omega) + \Sigma_t^0(\mathbf{r}) \delta\varphi(\mathbf{r}, \Omega) \quad (25)$$

and

$$\begin{aligned} A^{(1)} \psi^{(1)} \triangleq -\mathbf{\Omega} \cdot \nabla \psi^{(1)}(\mathbf{r}, \Omega) \\ + \Sigma_t^0(\mathbf{r}) \psi^{(1)}(\mathbf{r}, \Omega), \end{aligned} \quad (26)$$

and where the bilinear concomitant $P^{(1)}(\delta\varphi, \psi^{(1)})$ on the boundary $(\partial V \times \partial\Omega)$ is defined as

$$\begin{aligned} P^{(1)}(\delta\varphi, \psi^{(1)}) \triangleq \int_{\mathbf{\Omega} \cdot \mathbf{n} < 0} d\Omega \int_{\partial V} dA |\mathbf{\Omega} \cdot \mathbf{n}| \delta\varphi(\mathbf{r}, \Omega) \psi^{(1)}(\mathbf{r}, \Omega) \\ - \int_{\mathbf{\Omega} \cdot \mathbf{n} > 0} d\Omega \int_{\partial V} dA \mathbf{\Omega} \cdot \mathbf{n} \delta\varphi(\mathbf{r}, \Omega) \psi^{(1)}(\mathbf{r}, \Omega). \end{aligned} \quad (27)$$

Note that the superscript zero denoting nominal values will be omitted henceforth in order to simplify the notation. This simplification should not cause any loss of clarity, since it will become clear from the context which quantities are to be evaluated/computed using the nominal values for the model parameters.

4. Use Eq. (23) in conjunction with the boundary conditions given in Eq. (18) to construct the following 1st-LASS to be satisfied by the first-level adjoint function $\psi^{(1)}(r, \Omega)$:

$$A^{(1)}\psi^{(1)} \triangleq -\Omega \cdot \nabla\psi^{(1)}(\mathbf{r}, \Omega) + \Sigma_t(\mathbf{r})\psi^{(1)}(\mathbf{r}, \Omega) = \Sigma_d(\mathbf{r}, \Omega) , \tag{28}$$

together with the boundary condition

$$\psi^{(1)}(\mathbf{r}_s, \Omega) = 0 , \mathbf{r}_s \in \partial V , \Omega \cdot \mathbf{n} > 0 , \tag{29}$$

which is selected in order to cause the bilinear concomitant $P^{(1)}(\delta\phi, \psi^{(1)})$ in Eq. (24) to vanish.

5. Use the 1st-LFSS defined by Eqs. (17) and (18) together with Eqs. (25) and (26) to obtain the following expression for the indirect-effect term [see Eq. (16)], in terms of the first-level adjoint function $\psi^{(1)}(r, \Omega)$:

$$\left\{ \delta R(\phi, \mathbf{a}; \psi^{(1)}, \delta\mathbf{a}) \right\}_{ind} = \int dV \int_{4\pi} d\Omega \psi^{(1)}(\mathbf{r}, \Omega) [\delta q(\mathbf{r}) - \delta\Sigma_t(\mathbf{r})\phi(\mathbf{r}, \Omega)] . \tag{30}$$

As is well known, the 1st-LASS is solved by using the same numerical method as used for solving the original Eqs. (1) and (2), except for replacing Ω with $-\Omega$, and recognizing that the adjoint particles travel backward, i.e., in the $-\Omega$ direction. As is well known, the 1st-LASS is independent of parameter variations, so it needs to be solved just once for each particular form that the source term $\Sigma_d(\mathbf{r}, \Omega)$ might have to obtain the first-level adjoint function $\psi^{(1)}(\mathbf{r}, \Omega)$. The indirect-effect term is computed efficiently once $\psi^{(1)}(\mathbf{r}, \Omega)$ is available by performing the integrations (quadratures) indicated in Eq. (27).

Replacing Eqs. (30) and (15) in Eq. (14) yields the following expression for the total first-order response sensitivity in terms of the first-level adjoint function $\psi^{(1)}(\mathbf{r}, \Omega)$:

$$\delta R(\phi, \mathbf{a}; \psi^{(1)}, \delta\mathbf{a}) = \int dV \int_{4\pi} d\Omega \delta\Sigma_d(\mathbf{r}, \Omega)\phi(\mathbf{r}, \Omega) + \int dV \int_{4\pi} d\Omega \psi^{(1)}(r, \Omega) [\delta q(\mathbf{r}) - \delta\Sigma_t(\mathbf{r})\phi(\mathbf{r}, \Omega)] . \tag{31}$$

The partial first-order response sensitivity to a generic parameter α_i is obtained from Eq. (31) as

$$S_{m_1}^{(1)}(\phi, \mathbf{a}; \psi^{(1)}) \triangleq \frac{\partial R(\phi, \mathbf{a}; \psi^{(1)}, \delta\mathbf{a})}{\partial \alpha_{m_1}} = \sum_{k=1}^{N_d} \frac{\partial \mu_k(\mathbf{a})}{\partial \alpha_{m_1}} \int dV \int_{4\pi} d\Omega h_k(\mathbf{r}, \Omega)\phi(\mathbf{r}, \Omega) + \sum_{k=1}^{N_m} \frac{\partial Q_k(\mathbf{a})}{\partial \alpha_{m_1}} \int dV \int_{4\pi} d\Omega \psi^{(1)}(r, \Omega)g_k(\mathbf{r}) - \sum_{k=1}^{N_m} \frac{\partial C_k(\mathbf{a})}{\partial \alpha_{m_1}} \int dV \int_{4\pi} d\Omega \psi^{(1)}(r, \Omega)\phi(\mathbf{r}, \Omega)f_k(\mathbf{r}) , \tag{32}$$

$m_1 = 1, \dots, N_\alpha .$

In the illustrative examples presented in Secs. V, VI, and VII and in many other practical instances, the quantities $\Sigma_t(\mathbf{r})$, $q(\mathbf{r})$, and $\Sigma_d(\mathbf{r}, \Omega)$ can be represented as follows:

$$\Sigma_t(\mathbf{r}) = \sum_{j=1}^{N_m} N_j \sigma_j f_j(\mathbf{r}) , \tag{33}$$

$$q(\mathbf{r}) = \sum_{j=1}^{N_m} N_j q_j g_j(\mathbf{r}) , \tag{34}$$

and

$$\Sigma_d(\mathbf{r}, \Omega) = \sum_{k=1}^{N_d} \lambda_k h_k(\mathbf{r}, \Omega) . \tag{35}$$

The following definitions apply to Eqs. (33), (34), and (35):

1. N_j represents the atomic number density, σ_j denotes the microscopic cross section, and $f_j(\mathbf{r})$ denotes the spatial variation, respectively, which characterize the j 'th material contained in the heterogeneous medium under consideration, while N_m denotes the total number of materials contained in this medium.

2. q_j and $g_j(\mathbf{r})$ denote the source emission rate, and respectively, the spatial variation of the respective source contained in the j 'th material within the heterogeneous medium under consideration.

3. λ_k and $h_k(\mathbf{r}, \mathbf{\Omega})$ denote the scalar interaction coefficient of neutrons or gamma rays, and respectively, the corresponding spatial and angular variation of this interaction coefficient within the detector's k 'th material; the total number of distinct materials within the detector is denoted as N_d .

It follows from Eqs. (33), (34), and (35) that the variations $\delta q(\mathbf{r})$, $\delta \Sigma_t(\mathbf{r})$, and $\delta \Sigma_d(\mathbf{r}, \mathbf{\Omega})$ in the model parameters $\Sigma_t(\mathbf{r})$, $q(\mathbf{r})$, $\Sigma_d(\mathbf{r}, \mathbf{\Omega})$, respectively, have the following expressions:

$$\delta \Sigma_t(\mathbf{r}) = \sum_{j=1}^{N_m} [(\delta N_j) \sigma_j + (\delta \sigma_j) N_j] f_j(\mathbf{r}), \quad (36)$$

$$\delta q(\mathbf{r}) = \sum_{j=1}^{N_m} [(\delta N_j) q_j + (\delta q_j) N_j] g_j(\mathbf{r}), \quad (37)$$

and

$$\delta \Sigma_d(\mathbf{r}, \mathbf{\Omega}) = \sum_{k=1}^{N_d} (\delta \lambda_k) h_k(\mathbf{r}, \mathbf{\Omega}), \quad (38)$$

where the scalar-valued variations δN_j , $\delta \sigma_j$, δq_j , and $\delta \lambda_k$ are considered to be known. For bookkeeping purposes for this specific situation, it is convenient to consider that the model parameters N_j , σ_j , q_j , and λ_k are ordered as the components of a (column) vector of model parameters denoted as $\boldsymbol{\alpha}$ and defined as follows:

$$\boldsymbol{\alpha} \triangleq [\alpha_1, \dots, \alpha_{N_\alpha}]^\dagger, \quad (39a)$$

$$\alpha_j \triangleq N_j \text{ for } j = 1, \dots, N_m, \quad (39b)$$

$$\alpha_{N_m+j} \triangleq \sigma_j \text{ for } j = 1, \dots, N_m, \quad (39c)$$

$$\alpha_{2N_m+j} \triangleq q_j \text{ for } j = 1, \dots, N_m, \quad (39d)$$

$$\alpha_{3N_m+j} \triangleq \lambda_j \text{ for } j = 1, \dots, N_d, \quad (39e)$$

and

$$N_\alpha \triangleq 3N_m + N_d. \quad (39f)$$

Specializing Eq. (32) to the particular case described by Eqs. (36), (37), and (38) and identifying the terms corresponding to the various variations $\delta \boldsymbol{\alpha}$ yields the following expressions for the respective first-order partial sensitivities:

$$\begin{aligned} S_i^{(1)}(\varphi, \boldsymbol{\alpha}; \psi^{(1)}) &\triangleq \frac{\partial R}{\partial N_i} \\ &= -\sigma_i \int dV \int_{4\pi} d\boldsymbol{\Omega} f_i(\mathbf{r}) \psi^{(1)}(\mathbf{r}, \mathbf{\Omega}) \varphi(\mathbf{r}, \mathbf{\Omega}) \\ &\quad + q_i \int dV \int_{4\pi} d\boldsymbol{\Omega} \psi^{(1)}(r, \mathbf{\Omega}) g_i(\mathbf{r}), \\ i &= 1, \dots, N_m, \end{aligned} \quad (40)$$

$$\begin{aligned} S_{i+N_m}^{(1)}(\varphi, \boldsymbol{\alpha}; \psi^{(1)}) &\triangleq \frac{\partial R}{\partial \sigma_i} \\ &= -N_i \int dV \int_{4\pi} d\boldsymbol{\Omega} f_i(\mathbf{r}) \psi^{(1)}(\mathbf{r}, \mathbf{\Omega}) \varphi(\mathbf{r}, \mathbf{\Omega}), \\ i &= 1, \dots, N_m, \end{aligned} \quad (41)$$

$$\begin{aligned} S_{i+2N_m}^{(1)}(\boldsymbol{\alpha}; \psi^{(1)}) &\triangleq \frac{\partial R}{\partial q_i} = N_i \int dV \int_{4\pi} d\boldsymbol{\Omega} \psi^{(1)}(\mathbf{r}, \mathbf{\Omega}) g_i(\mathbf{r}), \\ i &= 1, \dots, N_m, \end{aligned} \quad (42)$$

and

$$\begin{aligned} S_{i+3N_m}^{(1)}(\varphi, \boldsymbol{\alpha}) &\triangleq \frac{\partial R}{\partial \lambda_i} = \int dV \int_{4\pi} d\boldsymbol{\Omega} \varphi(\mathbf{r}, \mathbf{\Omega}) h_i(\mathbf{r}, \mathbf{\Omega}), \\ i &= 1, \dots, N_d. \end{aligned} \quad (43)$$

The density derivatives here and everywhere in this paper are constant-volume partial derivatives.⁹

IV. SECOND-LEVEL FORWARD AND ADJOINT SENSITIVITY SYSTEMS FOR COMPUTING SECOND-ORDER RESPONSE SENSITIVITIES TO VARIATIONS IN MODEL PARAMETERS

The second-order response sensitivities will be denoted as $S_{m_1, m_2}^{(2)} \triangleq \frac{\partial^2 R}{\partial \alpha_{m_1} \partial \alpha_{m_2}}$, $m_1, m_2 = 1, \dots, N_\alpha$, and will be obtained by applying the 2nd-ASAM developed by Cacuci,^{1,2} which relies on the construction of a 2nd-LASS for each of the first-order sensitivities defined by Eq. (32). Thus, the G-differential of the first-order sensitivities defined in Eq. (32) yields the following expression:

$$\begin{aligned} \delta S_{m_1}^{(1)}(\varphi, \boldsymbol{\alpha}; \psi^{(1)}; \delta \boldsymbol{\alpha}) &= \left\{ \delta S_{m_1}^{(1)}(\varphi, \boldsymbol{\alpha}; \psi^{(1)}, \delta \boldsymbol{\alpha}) \right\}_{dir} \\ &\quad + \left\{ \delta S_{m_1}^{(1)}(\varphi, \boldsymbol{\alpha}; \psi^{(1)}, \delta \boldsymbol{\alpha}) \right\}_{ind}, \\ m_1 &= 1, \dots, N_\alpha, \end{aligned} \quad (44)$$

where

$$\begin{aligned} \left\{ \delta S_{m_1}^{(1)}(\varphi, \mathbf{\alpha}; \psi^{(1)}, \delta \mathbf{\alpha}) \right\}_{dir} &\triangleq \sum_{k=1}^{N_d} \sum_{j=1}^{N_\alpha} \frac{\partial^2 \mu_k(\mathbf{\alpha})}{\partial \alpha_{m_1} \partial \alpha_j} \delta \alpha_j \\ &\times \int dV \int_{4\pi} d\Omega h_k(\mathbf{r}, \Omega) \varphi(\mathbf{r}, \Omega) + \sum_{k=1}^{N_m} \sum_{j=1}^{N_\alpha} \frac{\partial^2 Q_k(\mathbf{\alpha})}{\partial \alpha_{m_1} \partial \alpha_j} \delta \alpha_j \\ &\times \int dV \int_{4\pi} d\Omega \psi^{(1)}(r, \Omega) g_k(\mathbf{r}) - \sum_{k=1}^{N_m} \sum_{j=1}^{N_\alpha} \frac{\partial^2 C_k(\mathbf{\alpha})}{\partial \alpha_{m_1} \partial \alpha_j} \delta \alpha_j \\ &\times \int dV \int_{4\pi} d\Omega \psi^{(1)}(r, \Omega) \varphi(\mathbf{r}, \Omega) f_k(\mathbf{r}), \quad m_1 = 1, \dots, N_\alpha \end{aligned} \quad (45)$$

and

$$\begin{aligned} \left\{ \delta S_{m_1}^{(1)}(\varphi, \mathbf{\alpha}; \psi^{(1)}, \delta \mathbf{\alpha}) \right\}_{ind} &\triangleq \sum_{k=1}^{N_d} \frac{\partial \mu_k(\mathbf{\alpha})}{\partial \alpha_{m_1}} \\ &\times \int dV \int_{4\pi} d\Omega h_k(\mathbf{r}, \Omega) \delta \varphi(\mathbf{r}, \Omega) + \sum_{k=1}^{N_m} \frac{\partial Q_k(\mathbf{\alpha})}{\partial \alpha_{m_1}} \\ &\times \int dV \int_{4\pi} d\Omega \delta \psi^{(1)}(r, \Omega) g_k(\mathbf{r}) - \sum_{k=1}^{N_m} \frac{\partial C_k(\mathbf{\alpha})}{\partial \alpha_{m_1}} \\ &\times \int dV \int_{4\pi} d\Omega \left[\delta \psi^{(1)}(r, \Omega) \varphi(\mathbf{r}, \Omega) \right. \\ &\left. + \psi^{(1)}(r, \Omega) \delta \varphi(\mathbf{r}, \Omega) \right] f_k(\mathbf{r}), \quad m_1 = 1, \dots, N_\alpha. \end{aligned} \quad (46)$$

The direct-effect term $\left\{ \delta S_{m_1}^{(1)}(\varphi, \mathbf{\alpha}; \psi^{(1)}, \delta \mathbf{\alpha}) \right\}_{dir}$ can be computed immediately. On the other hand, the indirect-effect term $\left\{ \delta S_{m_1}^{(1)}(\varphi, \mathbf{\alpha}; \psi^{(1)}, \delta \mathbf{\alpha}) \right\}_{ind}$ can be computed only after having obtained the variation $\delta \varphi(\mathbf{r}, \Omega)$ in the forward angular flux and the variation $\delta \psi^{(1)}(r, \Omega)$ in the first-level adjoint function. The function $\delta \psi^{(1)}(r, \Omega)$ is the solution of the system of equations obtained by G-differentiating the 1st-LASS, see Eqs. (28) and (29), which yields

$$\begin{aligned} -\Omega \cdot \nabla \delta \psi^{(1)}(\mathbf{r}, \Omega) + \Sigma_t(\mathbf{r}) \delta \psi^{(1)}(\mathbf{r}, \Omega) \\ = \delta \Sigma_d(\mathbf{r}, \Omega) - \delta \Sigma_t(\mathbf{r}) \psi^{(1)}(\mathbf{r}, \Omega) \end{aligned} \quad (47)$$

and

$$\delta \psi^{(1)}(\mathbf{r}_s, \Omega) = 0, \quad \mathbf{r}_s \in \partial V, \quad \Omega \cdot \mathbf{n} > 0. \quad (48)$$

It is evident from Eqs. (47) and (48) that the evaluation of the function $\delta \psi^{(1)}(\mathbf{r}, \Omega)$ is just as expensive computationally as determining the variation $\delta \varphi(\mathbf{r}, \Omega)$ by solving the 1st-LFSS. The system comprising Eqs. (47), (48), (17), and (18) is called^{1,2} the Second-Level Forward

Sensitivity System (2nd-LFSS). To avoid the need for solving the 2nd-LFSS, the indirect-effect term $\left\{ \delta S_{m_1}^{(1)}(\varphi, \mathbf{\alpha}; \psi^{(1)}, \delta \mathbf{\alpha}) \right\}_{ind}$ will be expressed in terms of the 2nd-LASS, which will be constructed by following the general principles introduced by Cacuci,^{1,2} comprising the following sequence of steps:

1. Define the inner product $\langle \mathbf{u}^{(2)}(\mathbf{r}, \Omega), \mathbf{w}^{(2)}(\mathbf{r}, \Omega) \rangle$ of two vector-valued functions $\mathbf{u}^{(2)}(\mathbf{r}, \Omega) \triangleq [u_1^{(2)}(\mathbf{r}, \Omega), u_2^{(2)}(\mathbf{r}, \Omega)]^\dagger$, with $u_1^{(2)}(\mathbf{r}, \Omega) \in L_2(V \times \Omega)$, $u_2^{(2)}(\mathbf{r}, \Omega) \in L_2(V \times \Omega)$, and $\mathbf{w}^{(2)}(\mathbf{r}, \Omega) \triangleq [w_1^{(2)}(\mathbf{r}, \Omega), w_2^{(2)}(\mathbf{r}, \Omega)]^\dagger$, with $w_1^{(2)}(\mathbf{r}, \Omega) \in L_2(V \times \Omega)$, $w_2^{(2)}(\mathbf{r}, \Omega) \in L_2(V \times \Omega)$, as follows:

$$\langle \mathbf{u}^{(2)}(\mathbf{r}, \Omega), \mathbf{w}^{(2)}(\mathbf{r}, \Omega) \rangle \triangleq \sum_{j=1}^2 \int dV \int_{4\pi} d\Omega u_j^{(2)}(\mathbf{r}, \Omega) w_j^{(2)}(\mathbf{r}, \Omega). \quad (49)$$

2. For matrix-valued linear operator $\mathbf{L}^{(2)} \triangleq \begin{pmatrix} L_{11}^{(2)} & L_{12}^{(2)} \\ L_{21}^{(2)} & L_{22}^{(2)} \end{pmatrix}$, define its formal adjoint operator $\mathbf{A}^{(2)} \triangleq \begin{pmatrix} A_{11}^{(2)} & A_{12}^{(2)} \\ A_{21}^{(2)} & A_{22}^{(2)} \end{pmatrix}$ through the following relationship:

$$\langle \mathbf{w}^{(2)}, \mathbf{L}^{(2)} \mathbf{u}^{(2)} \rangle = \langle \mathbf{u}^{(2)}, \mathbf{A}^{(2)} \mathbf{w}^{(2)} \rangle + P^{(2)}(\mathbf{u}^{(2)}, \mathbf{w}^{(2)}), \quad (50)$$

where $P^{(2)}(\mathbf{u}^{(2)}, \mathbf{w}^{(2)})$ denotes the corresponding bilinear concomitant on the boundary $(\partial V \times \partial \Omega)$.

3. Apply the definition provided in Eq. (49) to form the inner product of Eqs. (47) and (17) with a yet undefined function $\boldsymbol{\psi}_{m_1}^{(2)}(\mathbf{r}, \Omega) \triangleq [\psi_{1,m_1}^{(2)}(\mathbf{r}, \Omega), \psi_{2,m_1}^{(2)}(\mathbf{r}, \Omega)]^\dagger$, $\psi_{1,m_1}^{(2)}(\mathbf{r}, \Omega) \in L_2(V \times \Omega)$ and $\psi_{2,m_1}^{(2)}(\mathbf{r}, \Omega) \in L_2(V \times \Omega)$, to obtain

$$\begin{aligned} \int dV \int_{4\pi} d\Omega \boldsymbol{\psi}_{1,m_1}^{(2)}(\mathbf{r}, \Omega) \left[-\Omega \cdot \nabla \delta \psi^{(1)}(\mathbf{r}, \Omega) + \Sigma_t(\mathbf{r}) \delta \psi^{(1)}(\mathbf{r}, \Omega) \right] \\ + \int dV \int_{4\pi} d\Omega \boldsymbol{\psi}_{2,m_1}^{(2)}(\mathbf{r}, \Omega) \left[\Omega \cdot \nabla \delta \varphi(\mathbf{r}, \Omega) + \Sigma_t(\mathbf{r}) \delta \varphi(\mathbf{r}, \Omega) \right] \\ = \int dV \int_{4\pi} d\Omega \boldsymbol{\psi}_{1,m_1}^{(2)}(\mathbf{r}, \Omega) \left[\delta \Sigma_d(\mathbf{r}, \Omega) - \delta \Sigma_t(\mathbf{r}) \psi^{(1)}(\mathbf{r}, \Omega) \right] \\ + \int dV \int_{4\pi} d\Omega \boldsymbol{\psi}_{2,m_1}^{(2)}(\mathbf{r}, \Omega) \left[\delta q(\mathbf{r}) - \delta \Sigma_t(\mathbf{r}) \varphi(\mathbf{r}, \Omega) \right]. \end{aligned} \quad (51)$$

4. Apply Eq. (50) to the left side of Eq. (51) for the special case when $\mathbf{u}^{(2)}(\mathbf{r}, \boldsymbol{\Omega}) \triangleq [\delta\psi^{(1)}(\mathbf{r}, \boldsymbol{\Omega}), \delta\varphi(\mathbf{r}, \boldsymbol{\Omega})]^\dagger$, $\mathbf{w}^{(2)} \triangleq \boldsymbol{\psi}_{m_1}^{(2)}(\mathbf{r}, \boldsymbol{\Omega})$, $L_{12}^{(2)} = L_{21}^{(2)} \equiv 0$, $L_{11}^{(2)}\psi^{(1)} \triangleq -\boldsymbol{\Omega} \cdot \nabla\psi^{(1)}(\mathbf{r}, \boldsymbol{\Omega}) + \Sigma_t(\mathbf{r})\psi^{(1)}(\mathbf{r}, \boldsymbol{\Omega})$, and $L_{22}^{(2)}\delta\varphi \triangleq \boldsymbol{\Omega} \cdot \nabla\delta\varphi(\mathbf{r}, \boldsymbol{\Omega}) + \Sigma_t(\mathbf{r})\delta\varphi(\mathbf{r}, \boldsymbol{\Omega})$ to obtain

$$\begin{aligned} & \int dV \int_{4\pi} d\boldsymbol{\Omega} \psi_{1,m_1}^{(2)}(\mathbf{r}, \boldsymbol{\Omega}) \left[-\boldsymbol{\Omega} \cdot \nabla \delta\psi^{(1)}(\mathbf{r}, \boldsymbol{\Omega}) + \Sigma_t(\mathbf{r}) \delta\psi^{(1)}(\mathbf{r}, \boldsymbol{\Omega}) \right] \\ & + \int dV \int_{4\pi} d\boldsymbol{\Omega} \psi_{2,m_1}^{(2)}(\mathbf{r}, \boldsymbol{\Omega}) \left[\boldsymbol{\Omega} \cdot \nabla \delta\varphi(\mathbf{r}, \boldsymbol{\Omega}) + \Sigma_t(\mathbf{r}) \delta\varphi(\mathbf{r}, \boldsymbol{\Omega}) \right] \\ & = \int dV \int_{4\pi} d\boldsymbol{\Omega} \delta\psi^{(1)}(\mathbf{r}, \boldsymbol{\Omega}) \left[\boldsymbol{\Omega} \cdot \nabla \psi_{1,m_1}^{(2)}(\mathbf{r}, \boldsymbol{\Omega}) + \Sigma_t(\mathbf{r}) \psi_{1,m_1}^{(2)}(\mathbf{r}, \boldsymbol{\Omega}) \right] \\ & + \int dV \int_{4\pi} d\boldsymbol{\Omega} \delta\varphi(\mathbf{r}, \boldsymbol{\Omega}) \left[-\boldsymbol{\Omega} \cdot \nabla \psi_{2,m_1}^{(2)}(\mathbf{r}, \boldsymbol{\Omega}) + \Sigma_t(\mathbf{r}) \psi_{2,m_1}^{(2)}(\mathbf{r}, \boldsymbol{\Omega}) \right] \\ & + P^{(2)}(\mathbf{u}^{(2)}, \boldsymbol{\psi}_{m_1}^{(2)}). \end{aligned} \quad (52)$$

Equation (52) indicates that the components of the adjoint operator $\mathbf{A}^{(2)}$ are $A_{11}^{(2)}\psi^{(1)} \triangleq \boldsymbol{\Omega} \cdot \nabla\psi_{1,m_1}^{(2)}(\mathbf{r}, \boldsymbol{\Omega}) + \Sigma_t(\mathbf{r})\psi_{1,m_1}^{(2)}(\mathbf{r}, \boldsymbol{\Omega})$, $A_{12}^{(2)} = A_{21}^{(2)} \equiv 0$ and $A_{22}^{(2)}\delta\varphi \triangleq -\boldsymbol{\Omega} \cdot \nabla\psi_{2,m_1}^{(2)}(\mathbf{r}, \boldsymbol{\Omega}) + \Sigma_t(\mathbf{r})\psi_{2,m_1}^{(2)}(\mathbf{r}, \boldsymbol{\Omega})$.

5. Use the boundary conditions shown in Eqs. (18) and (48), and impose on $\boldsymbol{\psi}_{m_1}^{(2)}(\mathbf{r}, \boldsymbol{\Omega}) \triangleq [\psi_{1,m_1}^{(2)}(\mathbf{r}, \boldsymbol{\Omega}), \psi_{2,m_1}^{(2)}(\mathbf{r}, \boldsymbol{\Omega})]^\dagger$ the boundary conditions $\psi_{1,m_1}^{(2)}(\mathbf{r}, \boldsymbol{\Omega}) = 0, \mathbf{r}_s \in \partial V, \boldsymbol{\Omega} \cdot \mathbf{n} < 0$, and $\psi_{1,m_2}^{(2)}(\mathbf{r}, \boldsymbol{\Omega}) = 0, \mathbf{r}_s \in \partial V, \boldsymbol{\Omega} \cdot \mathbf{n} > 0$, to cause the bilinear concomitant $P^{(2)}(\mathbf{u}^{(2)}, \boldsymbol{\psi}_{m_1}^{(2)})$ in Eq. (52) to vanish.

6. Identify the right side of Eq. (52) with the indirect-effect term defined in Eq. (46) to obtain the following form of the 2nd-LASS to be used for computing the functions $\psi_{1,m_1}^{(2)}(\mathbf{r}, \boldsymbol{\Omega})$ and $\psi_{2,m_1}^{(2)}(\mathbf{r}, \boldsymbol{\Omega})$, $m_1 = 1, \dots, N_\alpha$, which will ultimately be used to evaluate Eq. (46):

$$\boldsymbol{\Omega} \cdot \nabla \psi_{1,m_1}^{(2)}(\mathbf{r}, \boldsymbol{\Omega}) + \Sigma_t(\mathbf{r})\psi_{1,m_1}^{(2)}(\mathbf{r}, \boldsymbol{\Omega}) = \sum_{k=1}^{N_m} \frac{\partial Q_k(\boldsymbol{\alpha})}{\partial \alpha_{m_1}} g_k(\mathbf{r}) - \varphi(\mathbf{r}, \boldsymbol{\Omega}) \sum_{k=1}^{N_m} \frac{\partial C_k(\boldsymbol{\alpha})}{\partial \alpha_{m_1}} f_k(\mathbf{r}), \quad (53)$$

$$\psi_{1,m_1}^{(2)}(\mathbf{r}_s, \boldsymbol{\Omega}) = 0, \mathbf{r}_s \in \partial V, \boldsymbol{\Omega} \cdot \mathbf{n} < 0, \quad (54)$$

$$-\boldsymbol{\Omega} \cdot \nabla \psi_{2,m_1}^{(2)}(\mathbf{r}, \boldsymbol{\Omega}) + \Sigma_t(\mathbf{r})\psi_{2,m_1}^{(2)}(\mathbf{r}, \boldsymbol{\Omega}) = \sum_{k=1}^{N_d} \frac{\partial \mu_k(\boldsymbol{\alpha})}{\partial \alpha_{m_1}} h_k(\mathbf{r}, \boldsymbol{\Omega}) - \psi^{(1)}(\mathbf{r}, \boldsymbol{\Omega}) \sum_{k=1}^{N_m} \frac{\partial C_k(\boldsymbol{\alpha})}{\partial \alpha_{m_1}} f_k(\mathbf{r}), \quad (55)$$

and

$$\psi_{2,m_1}^{(2)}(\mathbf{r}_s, \boldsymbol{\Omega}) = 0, \mathbf{r}_s \in \partial V, \boldsymbol{\Omega} \cdot \mathbf{n} > 0. \quad (56)$$

7. Use Eqs. (51) and (52) together with Eqs. (45), (46), (19), (20), and (21) in Eq. (44) to obtain the following expression for $\delta S_{m_1}^{(1)}(\varphi, \boldsymbol{\alpha}; \psi^{(1)}; \psi_{1,m_1}^{(2)}, \psi_{2,m_1}^{(2)}; \delta\boldsymbol{\alpha})$:

$$\begin{aligned} \delta S_{m_1}^{(1)}(\varphi, \boldsymbol{\alpha}; \psi^{(1)}; \psi_{1,m_1}^{(2)}, \psi_{2,m_1}^{(2)}; \delta\boldsymbol{\alpha}) & = \left\{ \delta S_{m_1}^{(1)}(\varphi, \boldsymbol{\alpha}; \psi^{(1)}, \delta\boldsymbol{\alpha}) \right\}_{dir} \\ & - \sum_{m_2=1}^{N_\alpha} \sum_{j=1}^{N_m} \frac{\partial C_j(\boldsymbol{\alpha})}{\partial \alpha_{m_2}} \delta\alpha_{m_2} \int dV \int_{4\pi} d\boldsymbol{\Omega} \left[\psi_{1,m_1}^{(2)}(\mathbf{r}, \boldsymbol{\Omega}) \psi^{(1)}(\mathbf{r}, \boldsymbol{\Omega}) + \psi_{2,m_1}^{(2)}(\mathbf{r}, \boldsymbol{\Omega}) \varphi(\mathbf{r}, \boldsymbol{\Omega}) \right] f_j(\mathbf{r}) \end{aligned}$$

$$\begin{aligned}
 & + \sum_{m_2=1}^{N_\alpha} \sum_{j=1}^{N_m} \frac{\partial Q_j(\boldsymbol{\alpha})}{\partial \alpha_{m_2}} \delta \alpha_{m_2} \int dV \int_{4\pi} d\boldsymbol{\Omega} \psi_{2,m_1}^{(2)}(\mathbf{r}, \boldsymbol{\Omega}) g_j(\mathbf{r}) \\
 & + \sum_{m_2=1}^{N_\alpha} \sum_{j=1}^{N_d} \frac{\partial \mu_j(\boldsymbol{\alpha})}{\partial \alpha_{m_2}} \delta \alpha_{m_2} \int dV \int_{4\pi} d\boldsymbol{\Omega} \psi_{1,m_1}^{(2)}(\mathbf{r}, \boldsymbol{\Omega}) h_j(\mathbf{r}, \boldsymbol{\Omega}), \quad m_1 = 1, \dots, N_\alpha.
 \end{aligned} \tag{57}$$

The second-order mixed partial sensitivities $S_{m_1, m_2}^{(2)} \triangleq \frac{\partial^2 R}{\partial \alpha_{m_1} \partial \alpha_{m_2}}$, $m_1, m_2 = 1, \dots, N_\alpha$, of the response with respect to the model parameters are determined by identifying in Eq. (57) the expressions multiplying the variations $\delta \alpha_{m_2}$. This identification yields

$$\begin{aligned}
 S_{m_1, m_2}^{(2)} & \triangleq \frac{\partial^2 R}{\partial \alpha_{m_1} \partial \alpha_{m_2}} = \sum_{j=1}^{N_m} \frac{\partial Q_j(\boldsymbol{\alpha})}{\partial \alpha_{m_2}} \int dV \int_{4\pi} d\boldsymbol{\Omega} \psi_{2,m_1}^{(2)}(\mathbf{r}, \boldsymbol{\Omega}) g_j(\mathbf{r}) \\
 & + \sum_{j=1}^{N_m} \frac{\partial^2 Q_j(\boldsymbol{\alpha})}{\partial \alpha_{m_1} \partial \alpha_{m_2}} \int dV \int_{4\pi} d\boldsymbol{\Omega} \psi^{(1)}(\mathbf{r}, \boldsymbol{\Omega}) g_j(\mathbf{r}) \\
 & + \sum_{j=1}^{N_d} \frac{\partial \mu_j(\boldsymbol{\alpha})}{\partial \alpha_{m_2}} \int dV \int_{4\pi} d\boldsymbol{\Omega} \psi_{1,m_1}^{(2)}(\mathbf{r}, \boldsymbol{\Omega}) h_j(\mathbf{r}, \boldsymbol{\Omega}) + \sum_{j=1}^{N_d} \frac{\partial^2 \mu_j(\boldsymbol{\alpha})}{\partial \alpha_{m_1} \partial \alpha_{m_2}} \int dV \int_{4\pi} h_j(\mathbf{r}, \boldsymbol{\Omega}) \varphi(\mathbf{r}, \boldsymbol{\Omega}) d\boldsymbol{\Omega} \\
 & - \sum_{j=1}^{N_m} \frac{\partial C_j(\boldsymbol{\alpha})}{\partial \alpha_{m_2}} \int dV \int_{4\pi} d\boldsymbol{\Omega} \left[\psi_{1,m_1}^{(2)}(\mathbf{r}, \boldsymbol{\Omega}) \psi^{(1)}(\mathbf{r}, \boldsymbol{\Omega}) + \psi_{2,m_1}^{(2)}(\mathbf{r}, \boldsymbol{\Omega}) \varphi(\mathbf{r}, \boldsymbol{\Omega}) \right] f_j(\mathbf{r}) \\
 & - \sum_{j=1}^{N_m} \frac{\partial^2 C_j(\boldsymbol{\alpha})}{\partial \alpha_{m_1} \partial \alpha_{m_2}} \int dV \int_{4\pi} d\boldsymbol{\Omega} \psi^{(1)}(\mathbf{r}, \boldsymbol{\Omega}) \varphi(\mathbf{r}, \boldsymbol{\Omega}) f_j(\mathbf{r}), \quad m_1, m_2 = 1, \dots, N_\alpha.
 \end{aligned} \tag{58}$$

In Secs. IV.A through IV.D, Eq. (58) will be specialized for the particular case described by Eqs. (40) through (43).

IV.A. Computation of the Second-Order Sensitivities $S_{i,j}^{(2)} \triangleq \frac{\partial^2 R}{\partial N_i \partial \alpha_j}$, $i = 1, \dots, N_m$, $j = 1, \dots, N_\alpha$

The second-order sensitivities $S_{i,j}^{(2)} \triangleq \frac{\partial^2 R}{\partial N_i \partial \alpha_j}$, $i = 1, \dots, N_m$, $j = 1, \dots, N_\alpha$ are obtained by computing the G-differential of the first-order sensitivities defined in Eq. (40), which yields

$$\delta S_i^{(1)}(\varphi, \boldsymbol{\alpha}; \psi^{(1)}; \delta \boldsymbol{\alpha}) = \left\{ \delta S_i^{(1)}(\varphi, \boldsymbol{\alpha}; \psi^{(1)}, \delta \boldsymbol{\alpha}) \right\}_{dir} + \left\{ \delta S_i^{(1)}(\varphi, \boldsymbol{\alpha}; \psi^{(1)}, \delta \boldsymbol{\alpha}) \right\}_{ind}, \quad i = 1, \dots, N_m, \tag{59}$$

where

$$\begin{aligned}
 \left\{ \delta S_i^{(1)}(\varphi, \boldsymbol{\alpha}; \psi^{(1)}, \delta \boldsymbol{\alpha}) \right\}_{dir} & \triangleq -\delta \sigma_i \int dV \int_{4\pi} d\boldsymbol{\Omega} f_i(\mathbf{r}) \psi^{(1)}(\mathbf{r}, \boldsymbol{\Omega}) \varphi(\mathbf{r}, \boldsymbol{\Omega}) \\
 & + \delta q_i \int dV \int_{4\pi} d\boldsymbol{\Omega} \psi^{(1)}(\mathbf{r}, \boldsymbol{\Omega}) g_i(\mathbf{r}), \quad i = 1, \dots, N_m
 \end{aligned} \tag{60}$$

and

$$\begin{aligned}
 \left\{ \delta S_i^{(1)}(\varphi, \boldsymbol{\alpha}; \psi^{(1)}, \delta \boldsymbol{\alpha}) \right\}_{ind} & \triangleq -\sigma_i \int dV \int_{4\pi} d\boldsymbol{\Omega} f_i(\mathbf{r}) \left[\delta \psi^{(1)}(\mathbf{r}, \boldsymbol{\Omega}) \varphi(\mathbf{r}, \boldsymbol{\Omega}) + \psi^{(1)}(\mathbf{r}, \boldsymbol{\Omega}) \delta \varphi(\mathbf{r}, \boldsymbol{\Omega}) \right] \\
 & + q_i \int dV \int_{4\pi} d\boldsymbol{\Omega} \delta \psi^{(1)}(\mathbf{r}, \boldsymbol{\Omega}) g_i(\mathbf{r}), \quad i = 1, \dots, N_m.
 \end{aligned} \tag{61}$$

Comparing Eqs. (60) and (61) to Eqs. (45) and (46), respectively, and following the general procedure outlined in the foregoing [which led to the general result given in Eq. (57)] yields the following expression for the right side of Eq. (59):

$$\begin{aligned} \delta S_i^{(1)}(\varphi, \boldsymbol{\alpha}; \psi^{(1)}; \psi_{1,i}^{(2)}, \psi_{2,i}^{(2)}; \delta \boldsymbol{\alpha}) = & - \int dV \int_{4\pi} d\boldsymbol{\Omega} \left[\psi_{1,i}^{(2)}(\mathbf{r}, \boldsymbol{\Omega}) \psi^{(1)}(\mathbf{r}, \boldsymbol{\Omega}) + \psi_{2,i}^{(2)}(\mathbf{r}, \boldsymbol{\Omega}) \varphi(\mathbf{r}, \boldsymbol{\Omega}) \right] \delta \Sigma_t(\mathbf{r}) \\ & + \int dV \int_{4\pi} d\boldsymbol{\Omega} \psi_{1,i}^{(2)}(\mathbf{r}, \boldsymbol{\Omega}) \delta \Sigma_d(\mathbf{r}, \boldsymbol{\Omega}) + \int dV \int_{4\pi} d\boldsymbol{\Omega} \psi_{2,i}^{(2)}(\mathbf{r}, \boldsymbol{\Omega}) \delta q(\mathbf{r}) \\ & - \delta \sigma_i \int dV \int_{4\pi} d\boldsymbol{\Omega} f_i(\mathbf{r}) \psi^{(1)}(\mathbf{r}, \boldsymbol{\Omega}) \varphi(\mathbf{r}, \boldsymbol{\Omega}) + \delta q_i \int dV \int_{4\pi} d\boldsymbol{\Omega} g_i(\mathbf{r}) \psi^{(1)}(\mathbf{r}, \boldsymbol{\Omega}), \\ & i = 1, \dots, N_m, \end{aligned} \quad (62)$$

where the second-level adjoint functions $\psi_{1,i}^{(2)}(\mathbf{r}, \boldsymbol{\Omega})$ and $\psi_{2,i}^{(2)}(\mathbf{r}, \boldsymbol{\Omega})$ are the solutions of the following 2nd-LASS:

$$\boldsymbol{\Omega} \cdot \nabla \psi_{1,i}^{(2)}(\mathbf{r}, \boldsymbol{\Omega}) + \Sigma_t(\mathbf{r}) \psi_{1,i}^{(2)}(\mathbf{r}, \boldsymbol{\Omega}) = -\sigma_i f_i(\mathbf{r}) \varphi(\mathbf{r}, \boldsymbol{\Omega}) + q_i g_i(\mathbf{r}), \quad i = 1, \dots, N_m, \quad (63)$$

$$\psi_{1,i}^{(2)}(\mathbf{r}_s, \boldsymbol{\Omega}) = 0, \mathbf{r}_s \in \partial V, \boldsymbol{\Omega} \cdot \mathbf{n} < 0, \quad (64)$$

$$-\boldsymbol{\Omega} \cdot \nabla \psi_{2,i}^{(2)}(\mathbf{r}, \boldsymbol{\Omega}) + \Sigma_t(\mathbf{r}) \psi_{2,i}^{(2)}(\mathbf{r}, \boldsymbol{\Omega}) = -\sigma_i f_i(\mathbf{r}) \psi^{(1)}(\mathbf{r}, \boldsymbol{\Omega}), \quad i = 1, \dots, N_m, \quad (65)$$

and

$$\psi_{2,i}^{(2)}(\mathbf{r}_s, \boldsymbol{\Omega}) = 0, \mathbf{r}_s \in \partial V, \boldsymbol{\Omega} \cdot \mathbf{n} > 0. \quad (66)$$

Replacing Eqs. (36), (37), and (38) in Eq. (62) and identifying the expressions multiplying the variations δN_j , $\delta \sigma_j$, δq_j , and $\delta \lambda_j$ yields the following expressions for (part of) the second-order mixed partial sensitivities of the response with respect to the model parameters:

$$\begin{aligned} S_{i,j}^{(2)} \triangleq \frac{\partial^2 R}{\partial N_i \partial N_j} = & -\sigma_j \int dV \int_{4\pi} d\boldsymbol{\Omega} \left[\psi_{1,i}^{(2)}(\mathbf{r}, \boldsymbol{\Omega}) \psi^{(1)}(\mathbf{r}, \boldsymbol{\Omega}) + \psi_{2,i}^{(2)}(\mathbf{r}, \boldsymbol{\Omega}) \varphi(\mathbf{r}, \boldsymbol{\Omega}) \right] f_j(\mathbf{r}) \\ & + q_j \int dV \int_{4\pi} d\boldsymbol{\Omega} \psi_{2,i}^{(2)}(\mathbf{r}, \boldsymbol{\Omega}) g_j(\mathbf{r}), \quad i, j = 1, \dots, N_m, \end{aligned} \quad (67)$$

$$\begin{aligned} S_{i,j+N_m}^{(2)} \triangleq \frac{\partial^2 R}{\partial N_i \partial \sigma_j} = & -N_j \int dV \int_{4\pi} d\boldsymbol{\Omega} \left[\psi_{1,i}^{(2)}(\mathbf{r}, \boldsymbol{\Omega}) \psi^{(1)}(\mathbf{r}, \boldsymbol{\Omega}) + \psi_{2,i}^{(2)}(\mathbf{r}, \boldsymbol{\Omega}) \varphi(\mathbf{r}, \boldsymbol{\Omega}) \right] f_j(\mathbf{r}) \\ & - \delta_{ij} \int dV \int_{4\pi} d\boldsymbol{\Omega} f_i(\mathbf{r}) \psi^{(1)}(\mathbf{r}, \boldsymbol{\Omega}) \varphi(\mathbf{r}, \boldsymbol{\Omega}), \quad i, j = 1, \dots, N_m, \end{aligned} \quad (68)$$

$$\begin{aligned} S_{i,j+2N_m}^{(2)} \triangleq \frac{\partial^2 R}{\partial N_i \partial q_j} = & N_j \int dV \int_{4\pi} d\boldsymbol{\Omega} \psi_{2,i}^{(2)}(\mathbf{r}, \boldsymbol{\Omega}) g_j(\mathbf{r}) + \delta_{ij} N_j \int dV \int_{4\pi} d\boldsymbol{\Omega} g_i(\mathbf{r}) \psi^{(1)}(\mathbf{r}, \boldsymbol{\Omega}), \\ & i, j = 1, \dots, N_m, \end{aligned} \quad (69)$$

and

$$S_{i,j+3N_m}^{(2)} \triangleq \frac{\partial^2 R}{\partial N_i \partial \lambda_j} = \int dV \int_{4\pi} d\boldsymbol{\Omega} \psi_{1,i}^{(2)}(\mathbf{r}, \boldsymbol{\Omega}) h_j(\mathbf{r}, \boldsymbol{\Omega}), \quad i = 1, \dots, N_m, \quad j = 1, \dots, N_d. \quad (70)$$

IV.B. Computation of the Second-Order Sensitivities $S_{i+N_m,j}^{(2)} \triangleq \frac{\partial^2 R}{\partial \sigma_i \partial \alpha_j}$, $i = 1, \dots, N_m$, $j = 1, \dots, N_a$

The second-order sensitivities $S_{i+N_m,j}^{(2)} \triangleq \frac{\partial^2 R}{\partial \sigma_i \partial \alpha_j}$, $i = 1, \dots, N_m$, $j = 1, \dots, N_a$ are obtained by computing the G-differential of the first-order sensitivities defined in Eq. (41), which yields

$$\delta S_{i+N_m}^{(1)}(\varphi, \boldsymbol{\alpha}; \boldsymbol{\psi}^{(1)}, \delta \boldsymbol{\alpha}) = \left\{ \delta S_{i+N_m}^{(1)}(\varphi, \boldsymbol{\alpha}; \boldsymbol{\psi}^{(1)}, \delta \boldsymbol{\alpha}) \right\}_{dir} + \left\{ \delta S_{i+N_m}^{(1)}(\varphi, \boldsymbol{\alpha}; \boldsymbol{\psi}^{(1)}, \delta \boldsymbol{\alpha}) \right\}_{ind}, \quad i = 1, \dots, N_m, \quad (71)$$

where

$$\left\{ \delta S_{i+N_m}^{(1)}(\varphi, \boldsymbol{\alpha}; \boldsymbol{\psi}^{(1)}, \delta \boldsymbol{\alpha}) \right\}_{dir} \triangleq -\delta N_i \int dV \int_{4\pi} d\boldsymbol{\Omega} f_i(\mathbf{r}) \boldsymbol{\psi}^{(1)}(\mathbf{r}, \boldsymbol{\Omega}) \varphi(\mathbf{r}, \boldsymbol{\Omega}), \quad i = 1, \dots, N_m \quad (72)$$

and

$$\begin{aligned} \left\{ \delta S_{i+N_m}^{(1)}(\varphi, \boldsymbol{\alpha}; \boldsymbol{\psi}^{(1)}, \delta \boldsymbol{\alpha}) \right\}_{ind} &\triangleq -N_i \int dV \int_{4\pi} d\boldsymbol{\Omega} f_i(\mathbf{r}) \delta \boldsymbol{\psi}^{(1)}(\mathbf{r}, \boldsymbol{\Omega}) \varphi(\mathbf{r}, \boldsymbol{\Omega}) \\ &- N_i \int dV \int_{4\pi} d\boldsymbol{\Omega} f_i(\mathbf{r}) \boldsymbol{\psi}^{(1)}(\mathbf{r}, \boldsymbol{\Omega}) \delta \varphi(\mathbf{r}, \boldsymbol{\Omega}), \quad i = 1, \dots, N_m. \end{aligned} \quad (73)$$

Comparing Eqs. (72) and (73) to Eqs. (45) and (46), respectively, and following the general procedure outlined in the foregoing [which led to the general result given in Eq. (57)] yields the following expression for the right side of Eq. (71):

$$\begin{aligned} \delta S_{i+N_m}^{(1)}(\varphi, \boldsymbol{\alpha}; \boldsymbol{\psi}^{(1)}; \boldsymbol{\psi}_{1,i+N_m}^{(2)}, \boldsymbol{\psi}_{2,i+N_m}^{(2)}; \delta \boldsymbol{\alpha}) &= -\delta N_i \int dV \int_{4\pi} d\boldsymbol{\Omega} f_i(\mathbf{r}) \boldsymbol{\psi}^{(1)}(\mathbf{r}, \boldsymbol{\Omega}) \varphi(\mathbf{r}, \boldsymbol{\Omega}) \\ &- \int dV \int_{4\pi} d\boldsymbol{\Omega} \left[\boldsymbol{\psi}_{1,i+N_m}^{(2)}(\mathbf{r}, \boldsymbol{\Omega}) \boldsymbol{\psi}^{(1)}(\mathbf{r}, \boldsymbol{\Omega}) + \boldsymbol{\psi}_{2,i+N_m}^{(2)}(\mathbf{r}, \boldsymbol{\Omega}) \varphi(\mathbf{r}, \boldsymbol{\Omega}) \right] \delta \Sigma_t(\mathbf{r}) \\ &+ \int dV \int_{4\pi} d\boldsymbol{\Omega} \boldsymbol{\psi}_{1,i+N_m}^{(2)}(\mathbf{r}, \boldsymbol{\Omega}) \delta \Sigma_d(\mathbf{r}, \boldsymbol{\Omega}) \\ &+ \int dV \int_{4\pi} d\boldsymbol{\Omega} \boldsymbol{\psi}_{2,i+N_m}^{(2)}(\mathbf{r}, \boldsymbol{\Omega}) \delta q(\mathbf{r}), \quad i = 1, \dots, N_m. \end{aligned} \quad (74)$$

The second-level adjoint functions $\boldsymbol{\psi}_{1,i+N_m}^{(2)}$ and $\boldsymbol{\psi}_{2,i+N_m}^{(2)}$ are the solutions of the following 2nd-LASS:

$$\boldsymbol{\Omega} \cdot \nabla \boldsymbol{\psi}_{1,i+N_m}^{(2)}(\mathbf{r}, \boldsymbol{\Omega}) + \Sigma_t(\mathbf{r}) \boldsymbol{\psi}_{1,i+N_m}^{(2)}(\mathbf{r}, \boldsymbol{\Omega}) = -N_i f_i(\mathbf{r}) \varphi(\mathbf{r}, \boldsymbol{\Omega}), \quad i = 1, \dots, N_m, \quad (75)$$

$$\boldsymbol{\psi}_{1,i+N_m}^{(2)}(\mathbf{r}_s, \boldsymbol{\Omega}) = 0, \quad \mathbf{r}_s \in \partial V, \quad \boldsymbol{\Omega} \cdot \mathbf{n} < 0, \quad (76)$$

$$-\boldsymbol{\Omega} \cdot \nabla \boldsymbol{\psi}_{2,i+N_m}^{(2)}(\mathbf{r}, \boldsymbol{\Omega}) + \Sigma_t(\mathbf{r}) \boldsymbol{\psi}_{2,i+N_m}^{(2)}(\mathbf{r}, \boldsymbol{\Omega}) = -N_i f_i(\mathbf{r}) \boldsymbol{\psi}^{(1)}(\mathbf{r}, \boldsymbol{\Omega}), \quad i = 1, \dots, N_m, \quad (77)$$

and

$$\boldsymbol{\psi}_{2,i+N_m}^{(2)}(\mathbf{r}_s, \boldsymbol{\Omega}) = 0, \quad \mathbf{r}_s \in \partial V, \quad \boldsymbol{\Omega} \cdot \mathbf{n} > 0. \quad (78)$$

Replacing Eqs. (36), (37), and (38) in Eq. (74) and identifying the expressions multiplying the variations δN_j , $\delta \sigma_j$, δq_j , and $\delta \lambda_j$ yields

$$\begin{aligned} S_{i+N_m,j}^{(2)} &\triangleq \frac{\partial^2 R}{\partial \sigma_i \partial N_j} = -\sigma_j \int dV \int_{4\pi} d\boldsymbol{\Omega} \left[\boldsymbol{\psi}_{1,i+N_m}^{(2)}(\mathbf{r}, \boldsymbol{\Omega}) \boldsymbol{\psi}^{(1)}(\mathbf{r}, \boldsymbol{\Omega}) + \boldsymbol{\psi}_{2,i+N_m}^{(2)}(\mathbf{r}, \boldsymbol{\Omega}) \varphi(\mathbf{r}, \boldsymbol{\Omega}) \right] f_j(\mathbf{r}) \\ &+ q_j \int dV \int_{4\pi} d\boldsymbol{\Omega} \boldsymbol{\psi}_{2,i+N_m}^{(2)}(\mathbf{r}, \boldsymbol{\Omega}) g_j(\mathbf{r}) - \delta_{ij} \int dV \int_{4\pi} d\boldsymbol{\Omega} f_i(\mathbf{r}) \boldsymbol{\psi}^{(1)}(\mathbf{r}, \boldsymbol{\Omega}) \varphi(\mathbf{r}, \boldsymbol{\Omega}), \quad i, j = 1, \dots, N_m, \end{aligned} \quad (79)$$

$$\begin{aligned} S_{i+N_m,j+N_m}^{(2)} &\triangleq \frac{\partial^2 R}{\partial \sigma_i \partial \sigma_j} \\ &= -N_j \int dV \int_{4\pi} d\boldsymbol{\Omega} \left[\boldsymbol{\psi}_{1,i+N_m}^{(2)}(\mathbf{r}, \boldsymbol{\Omega}) \boldsymbol{\psi}^{(1)}(\mathbf{r}, \boldsymbol{\Omega}) + \boldsymbol{\psi}_{2,i+N_m}^{(2)}(\mathbf{r}, \boldsymbol{\Omega}) \varphi(\mathbf{r}, \boldsymbol{\Omega}) \right] f_j(\mathbf{r}), \quad i, j = 1, \dots, N_m, \end{aligned} \quad (80)$$

$$S_{i+N_m, j+2N_m}^{(2)} \triangleq \frac{\partial^2 R}{\partial \sigma_i \partial q_j} = N_j \int dV \int_{4\pi} d\Omega \psi_{2, i+N_m}^{(2)}(\mathbf{r}, \Omega) g_j(\mathbf{r}),$$

$$i, j = 1, \dots, N_m, \quad (81)$$

and

$$S_{i+N_m, j+3N_m}^{(2)} \triangleq \frac{\partial^2 R}{\partial \sigma_i \partial \lambda_j} = \int dV \int_{4\pi} d\Omega \psi_{1, i+N_m}^{(2)}(\mathbf{r}, \Omega) h_j(\mathbf{r}, \Omega),$$

$$i = 1, \dots, N_m, \quad j = 1, \dots, N_d. \quad (82)$$

IV.C. Computation of the Second-Order Sensitivities

$$S_{i+2N_m, j}^{(2)} \triangleq \frac{\partial^2 R}{\partial q_i \partial \alpha_j}, \quad i = 1, \dots, N_m, \quad j = 1, \dots, N_\alpha$$

The second-order sensitivities $S_{i+2N_m, j}^{(2)} \triangleq \frac{\partial^2 R}{\partial q_i \partial \alpha_j}$, $i = 1, \dots, N_m$, $j = 1, \dots, N_\alpha$ are obtained by computing the G-differential of Eq. (42), which yields the following expression:

$$\delta S_{i+2N_m}^{(1)}(\varphi, \mathbf{a}; \psi^{(1)}, \delta \mathbf{a}) = \left\{ \delta S_{i+2N_m}^{(1)}(\varphi, \mathbf{a}; \psi^{(1)}, \delta \mathbf{a}) \right\}_{dir}$$

$$+ \left\{ \delta S_{i+2N_m}^{(1)}(\varphi, \mathbf{a}; \psi^{(1)}, \delta \mathbf{a}) \right\}_{ind}, \quad i = 1, \dots, N_m, \quad (83)$$

where

$$\left\{ \delta S_{i+2N_m}^{(1)}(\varphi, \mathbf{a}; \psi^{(1)}, \delta \mathbf{a}) \right\}_{dir}$$

$$\triangleq \delta N_i \int dV \int_{4\pi} d\Omega \psi^{(1)}(\mathbf{r}, \Omega) g_i(\mathbf{r}), \quad i = 1, \dots, N_m \quad (84)$$

and

$$\left\{ \delta S_{i+2N_m}^{(1)}(\varphi, \mathbf{a}; \psi^{(1)}, \delta \mathbf{a}) \right\}_{ind}$$

$$= N_i \int dV \int_{4\pi} d\Omega \delta \psi^{(1)}(\mathbf{r}, \Omega) g_i(\mathbf{r}), \quad i = 1, \dots, N_m. \quad (85)$$

Comparing Eqs. (84) and (85) to Eqs. (45) and (46), respectively, and following the general procedure outlined in the foregoing [which led to the general result given in Eq. (57)] yields the following expression for the right side of Eq. (85):

$$\left\{ \delta S_{i+2N_m}^{(1)}(\mathbf{a}; \psi^{(1)}; \psi_{1, i+2N_m}^{(2)}; \delta \mathbf{a}) \right\}_{ind} =$$

$$- \int dV \int_{4\pi} d\Omega \psi_{1, i+2N_m}^{(2)}(\mathbf{r}, \Omega) \psi^{(1)}(\mathbf{r}, \Omega) \delta \Sigma_t(\mathbf{r})$$

$$+ \int dV \int_{4\pi} d\Omega \psi_{1, i+2N_m}^{(2)}(\mathbf{r}, \Omega) \delta \Sigma_d(\mathbf{r}, \Omega), \quad (86)$$

where the second-level adjoint function $\psi_{1, i+2N_m}^{(2)}$ is the solution of the following 2nd-LASS:

$$\Omega \cdot \nabla \psi_{1, i+2N_m}^{(2)}(\mathbf{r}, \Omega) + \Sigma_t(\mathbf{r}) \psi_{1, i+2N_m}^{(2)}(\mathbf{r}, \Omega)$$

$$= N_i g_i(\mathbf{r}), \quad i = 1, \dots, N_m \quad (87)$$

and

$$\psi_{1, i+2N_m}^{(2)}(\mathbf{r}_s, \Omega) = 0, \quad \mathbf{r}_s \in \partial V, \quad \Omega \cdot \mathbf{n} < 0. \quad (88)$$

Note also that $\psi_{2, i+2N_m}^{(2)} \equiv 0$. Replacing Eqs. (36), (37), and (38) in Eq. (86) and identifying the expressions multiplying the variations δN_j , $\delta \sigma_j$, δq_j , and $\delta \lambda_j$ yields

$$S_{i+2N_m, j}^{(2)} \triangleq \frac{\partial^2 R}{\partial q_i \partial N_j} =$$

$$- \sigma_j \int dV \int_{4\pi} d\Omega \psi_{1, i+2N_m}^{(2)}(\mathbf{r}, \Omega) \psi^{(1)}(\mathbf{r}, \Omega) f_j(\mathbf{r})$$

$$+ \delta_{ij} \int dV \int_{4\pi} d\Omega \psi^{(1)}(\mathbf{r}, \Omega) g_i(\mathbf{r}),$$

$$i, j = 1, \dots, N_m, \quad (89)$$

$$S_{i+2N_m, j+N_m}^{(2)} \triangleq \frac{\partial^2 R}{\partial q_i \partial \sigma_j} =$$

$$- N_j \int dV \int_{4\pi} d\Omega \psi_{1, i+2N_m}^{(2)}(\mathbf{r}, \Omega) \psi^{(1)}(\mathbf{r}, \Omega) f_j(\mathbf{r}),$$

$$i, j = 1, \dots, N_m, \quad (90)$$

$$S_{i+2N_m, j+2N_m}^{(2)} \triangleq \frac{\partial^2 R}{\partial q_i \partial q_j} = 0, \quad i, j = 1, \dots, N_m, \quad (91)$$

and

$$S_{i+2N_m, j+3N_m}^{(2)} \triangleq \frac{\partial^2 R}{\partial q_i \partial \lambda_j} =$$

$$\int dV \int_{4\pi} d\Omega \psi_{1, i+2N_m}^{(2)}(\mathbf{r}, \Omega) h_j(\mathbf{r}, \Omega),$$

$$i = 1, \dots, N_m, \quad j = 1, \dots, N_d. \quad (92)$$

IV.D. Computation of the Second-Order Sensitivities

$$S_{i+3N_m, j}^{(2)} \triangleq \frac{\partial^2 R}{\partial \lambda_i \partial \alpha_j}, \quad i = 1, \dots, N_d, j = 1, \dots, N_\alpha$$

Note from Eq. (43) that the sensitivities $S_{i+3N_m}^{(1)}(\varphi, \alpha)$ do not display explicit dependence on the model parameters. The second-order sensitivities $S_{i+3N_m, j}^{(2)} \triangleq \frac{\partial^2 R}{\partial \lambda_i \partial \alpha_j}$, $i = 1, \dots, N_d, j = 1, \dots, N_\alpha$ are obtained by computing the G-differential of Eq. (43), which yields the following expression:

$$\delta S_{i+3N_m}^{(1)}(\alpha; \delta\varphi, \delta\alpha) = \int dV \int_{4\pi} d\Omega \delta\varphi(\mathbf{r}, \Omega) h_i(\mathbf{r}, \Omega), \quad i = 1, \dots, N_d. \quad (93)$$

Comparing Eq. (93) to Eq. (41) indicates that, by following the procedure outlined in Secs. IV.A, IV.B, and IV.C, the indirect-effect term in Eq. (93) will ultimately have the expression:

$$\begin{aligned} \delta S_{i+3N_m}^{(1)}(\alpha; \varphi, \psi_{2, i+3N_m}^{(2)}; \delta\alpha) = & \\ & - \int dV \int_{4\pi} d\Omega \psi_{2, i+3N_m}^{(2)}(\mathbf{r}, \Omega) \varphi(\mathbf{r}, \Omega) \delta\Sigma_i(\mathbf{r}) \\ & + \int dV \int_{4\pi} d\Omega \psi_{2, i+3N_m}^{(2)}(\mathbf{r}, \Omega) \delta q(\mathbf{r}), \end{aligned} \quad (94)$$

where the second-level adjoint function $\psi_{2, i+3N_m}^{(2)}$ is the solution of the following 2nd-LASS:

$$-\mathbf{\Omega} \cdot \nabla \psi_{2, i+3N_m}^{(2)}(\mathbf{r}, \Omega) + \Sigma_i(\mathbf{r}) \psi_{2, i+3N_m}^{(2)}(\mathbf{r}, \Omega) = h_i(\mathbf{r}, \Omega), \quad i = 1, \dots, N_d \quad (95)$$

and

$$\psi_{2, i+3N_m}^{(2)}(\mathbf{r}_s, \Omega) = 0, \quad \mathbf{r}_s \in \partial V, \mathbf{\Omega} \cdot \mathbf{n} > 0. \quad (96)$$

Note that $\psi_{1, i+3N_m}^{(2)} \equiv 0$. Replacing Eqs. (36), (37), and (38) in Eq. (94) and identifying the expressions multiplying the variations δN_j , $\delta\sigma_j$, δq_j , and $\delta\lambda_j$ yields

$$\begin{aligned} S_{i+3N_m, j}^{(2)} \triangleq \frac{\partial^2 R}{\partial \lambda_i \partial N_j} = & \\ & - \sigma_j \int dV \int_{4\pi} d\Omega \psi_{2, i+3N_m}^{(2)}(\mathbf{r}, \Omega) \varphi(\mathbf{r}, \Omega) f_j(\mathbf{r}) \\ & + q_j \int dV \int_{4\pi} d\Omega \psi_{2, i+3N_m}^{(2)}(\mathbf{r}, \Omega) g_j(\mathbf{r}), \end{aligned} \quad (97)$$

$$i = 1, \dots, N_d, j = 1, \dots, N_m,$$

$$\begin{aligned} S_{i+3N_m, j+N_m}^{(2)} \triangleq \frac{\partial^2 R}{\partial \lambda_i \partial \sigma_j} & \\ = -N_j \int dV \int_{4\pi} d\Omega \psi_{2, i+3N_m}^{(2)}(\mathbf{r}, \Omega) \varphi(\mathbf{r}, \Omega) f_j(\mathbf{r}), & \\ i = 1, \dots, N_d, j = 1, \dots, N_m, & \end{aligned} \quad (98)$$

$$\begin{aligned} S_{i+3N_m, j+2N_m}^{(2)} \triangleq \frac{\partial^2 R}{\partial \lambda_i \partial q_j} & \\ = N_j \int dV \int_{4\pi} d\Omega \psi_{2, i+3N_m}^{(2)}(\mathbf{r}, \Omega) g_j(\mathbf{r}), & \\ i = 1, \dots, N_d, j = 1, \dots, N_m, & \end{aligned} \quad (99)$$

and

$$S_{i+3N_m, j+3N_m}^{(2)} \triangleq \frac{\partial^2 R}{\partial \lambda_i \partial \lambda_j} = 0, \quad i = 1, \dots, N_d, j = 1, \dots, N_d. \quad (100)$$

IV.E. Discussion

The following conclusions can be drawn based on the results that have been presented in this section:

1. As is well known, a single 1st-LASS needs to be solved in order to compute all first-order response sensitivities to all N_α model parameters.

2. For each model parameter, a single 2nd-LASS needs to be solved for computing the corresponding mixed second-order sensitivities. Hence, computing all of the $N_\alpha(N_\alpha + 1)/2$ second-order sensitivities could require solving at most N_α 2nd-LASSs.

3. The solution of each of the 2nd-LASSs is a two-component vector-valued second-level adjoint function, except for the 2nd-LASS that corresponds to parameters that appear linearly in the response under consideration, in which case the vector-valued second-level adjoint function may have a null component.

4. Solving each of the 2nd-LASSs involves the inversion of the same operators as need to be inverted for solving the original transport equation and/or the 1st-LASS. Only the various source terms on the right sides of the 2nd-LASSs differ from each other, and they form the forward and/or 1st-LASS. Therefore, the same software can be used to solve both the 1st-LASS and the 2nd-LASS.

5. The computation of the second-order sensitivities involves the evaluations of integrals of the same form as those needed for computing the first-order sensitivities. Therefore, the same software can be used for computing both the first-order and second-order sensitivities.

6. Each of the mixed second-order sensitivities is computed twice, using two distinct second-level adjoint functions. Consequently, the 2nd-ASAM possesses an inherent solution verification mechanism that enables and ensures the accuracy verification of the solutions of all of the 2nd-LASSs.

7. As expected, the angular flux solution of the uncollided-flux problem is separately linear in the source strengths and detector interaction coefficients. This fact has been confirmed by the vanishing of the respective second-order unmixed sensitivities, as demonstrated by the results presented in Eqs. (91) and (100), respectively. In such cases, each of the respective vector-valued second-level adjoint functions will have an identically null component. Similar results have been obtained by Cacuci² for a benchmark problem modeling the linear neutron diffusion equation.

V. SPHERICAL TEST PROBLEM (ANALYTIC)

The analytic homogeneous spherical test problem is described generically in Sec. V.A and specific values used in this paper are given in Sec. V.B. Analytic values of the derivatives are presented in Sec. V.C. Derivatives computed by solving the 2nd-LASS using PARTISN are compared with the analytic values in Sec. V.D. Sensitivities given in Secs. IV.A, IV.B, and IV.C were computed and are presented in this section; sensitivities to the detector parameters (Sec. IV.D) were not computed.

V.A. Problem Setup

Consider a homogeneous sphere of radius a . The material consists of two isotopes with number densities

N_1 and N_2 . The microscopic cross sections for the two isotopes are σ_1 and σ_2 . Isotope 1 is a decay gamma-ray source; the line emission rate (per atom of isotope 1 per second) is q_1 . Isotope 2 may emit gamma rays, but not in the same line as isotope 1; q_2 is zero. Gamma rays are emitted isotropically.

The macroscopic cross-section Σ of the material is

$$\Sigma = \sigma_1 N_1 + \sigma_2 N_2. \quad (101)$$

The line source rate density q is

$$q = q_1 N_1. \quad (102)$$

The isotopic number densities are related to the material mass density ρ via

$$N_i = \frac{\rho w_i N_A}{A_i}, \quad i = 1, 2, \quad (103)$$

where

w_i = weight fraction of isotope i

A_i = atomic weight of isotope i

N_A = Avogadro's number.

The weight fractions satisfy the normalization $w_1 + w_2 = 1$. Whenever the mass density is perturbed in this problem, both number densities are perturbed according to Eq. (103). Weight fraction perturbations are not considered in this problem.

The uncollided escape probability P is^{6,10}

$$P = \frac{3}{8(\Sigma a)^3} \left[2(\Sigma a)^2 - 1 + (1 + 2\Sigma a)e^{-2\Sigma a} \right]. \quad (104)$$

The uncollided leakage from the sphere is the escape probability multiplied by the total source rate.⁷ The total source rate Q is the source rate density q of Eq. (102) multiplied by the volume V of the sphere:

$$Q = qV = q_1 N_1 V. \quad (105)$$

The uncollided leakage L is

$$L = QP. \quad (106)$$

We will need derivatives of P with respect to Σ . The first derivative is

$$\begin{aligned} \frac{\partial P}{\partial \Sigma} &= \frac{3(-3)}{8(\Sigma a)^3 \Sigma} \left[2(\Sigma a)^2 - 1 + (1 + 2\Sigma a)e^{-2\Sigma a} \right] \\ &\quad + \frac{3}{8(\Sigma a)^3} \left[4\Sigma a^2 + 2ae^{-2\Sigma a} - 2a(1 + 2\Sigma a)e^{-2\Sigma a} \right] \\ &= -\frac{3}{\Sigma} \left\{ P - \frac{1}{2\Sigma a} (1 - e^{-2\Sigma a}) \right\}. \end{aligned} \tag{107}$$

The second derivative of P with respect to Σ is

$$\begin{aligned} \frac{\partial^2 P}{\partial \Sigma^2} &= \frac{3}{\Sigma^2} P - \frac{3}{\Sigma} \frac{\partial P}{\partial \Sigma} - \frac{3}{\Sigma^3 a} (1 - e^{-2\Sigma a}) + \frac{3}{\Sigma^2} e^{-2\Sigma a} \\ &= \frac{3}{\Sigma^2} P - \frac{3}{\Sigma} \frac{\partial P}{\partial \Sigma} - \frac{3}{\Sigma^3 a} (1 - e^{-2\Sigma a} - \Sigma a e^{-2\Sigma a}) \\ &= \frac{3}{\Sigma^2} \left\{ P - \Sigma \frac{\partial P}{\partial \Sigma} - \frac{1}{\Sigma a} [1 - (1 + \Sigma a)e^{-2\Sigma a}] \right\}. \end{aligned} \tag{108}$$

Derivatives of the leakage [Eq. (106)] with respect to atom density, cross section, and source emission rate are derived in the Appendix.

The detector response function for this problem is a modification of Eq. (5):

$$\Sigma_d(\mathbf{r}, \Omega) = \Omega \cdot \mathbf{n} \delta(\mathbf{r} - \mathbf{r}_s), \quad \mathbf{r}_s \in \partial V, \tag{109}$$

where \mathbf{n} is the outward unit normal at each \mathbf{r}_s .

V.B. Problem Parameters

The material in the sphere has the parameters shown in Table I. Isotope 1 is ^{239}Pu and isotope 2 is ^{240}Pu . The total macroscopic cross sections and source rate density from Eqs. (1) and (102), respectively, for the material are also shown in Table I. The cross sections and source rate correspond to the 646-keV gamma-ray line from ^{239}Pu . The cross sections were obtained from the MCPLIB04 ACE-formatted photon cross-section library, which is distributed with MCNP, and do not contain coherent scattering. The source emission rate q_1 is from Gunnick et al.¹¹

The sphere radius is $a = 3.794$ cm.

V.C. Analytic Results

The escape probability, its derivatives, and the leakage are shown in Table II.

Derivatives of the leakage with respect to atom densities, cross sections, source emission rates, and the material density are shown in Tables III, IV, V, and VI,

TABLE I
Sphere and Material Parameters*

Parameter	Value
a	3.794 cm
ρ	15.8 g/cm ³
w_1	0.94
w_2	0.06
N_1	3.74142E-02 atoms/(b·cm)
N_2	2.37817E-03 atoms/(b·cm)
σ_1	5.27263E+01 b
σ_2	5.27263E+01 b
q_1	1.341E+05 $\gamma/(10^{24}$ atoms·s)
q_2	0 $\gamma/(\text{atom}\cdot\text{s})$
Σ	2.09810E+00/cm
q	5.01724E+03 $\gamma/(\text{cm}^3\cdot\text{s})$

*All numerical results used more digits for atom densities and cross sections than are presented here.

respectively. The mixed derivatives are shown in Table VII.

V.D. PARTISN Results Compared to Analytic Results

The equations of the 2nd-LASS derived in Sec. III were also solved using PARTISN (Ref. 8), an off-the-shelf discrete-ordinates code. These equations [namely, Eqs. (63) through (66), (75) through (78), (87), (88), (95), and (96)] have sources that are the angular flux solutions

TABLE II
Escape Probability, Its Derivatives, and the Leakage

Parameter	Value
P	9.34752E-02
$\partial P/\partial \Sigma$	-4.38435E-02 cm
$\partial^2 P/\partial \Sigma^2$	4.07803E-02 cm ²
L	1.07286E+05 γ/s

TABLE III
Derivatives of the Leakage with Respect to Atom Densities

Parameter	Value
$\partial L/\partial N_1$	2.14263E+05 $\gamma/s/[\text{atoms}/(\text{b}\cdot\text{cm})]$
$\partial^2 L/\partial N_1^2$	-1.17096E+07 $\gamma/s/[\text{atoms}/(\text{b}\cdot\text{cm})]^2$
$\partial L/\partial N_2$	-2.65325E+06 $\gamma/s/[\text{atoms}/(\text{b}\cdot\text{cm})]$
$\partial^2 L/\partial N_2^2$	1.30122E+08 $\gamma/s/[\text{atoms}/(\text{b}\cdot\text{cm})]^2$
$\partial^2 L/\partial N_1 \partial N_2$	5.92062E+07 $\gamma/s/[\text{atoms}/(\text{b}\cdot\text{cm})]^2$

TABLE IV

Derivatives of the Leakage with Respect to Cross Sections

Parameter	Value
$\partial L/\partial\sigma_1$	-1.88273E+03 $\gamma/s/b$
$\partial^2 L/\partial\sigma_1^2$	6.55191E+01 $\gamma/s/b^2$
$\partial L/\partial\sigma_2$	-1.19673E+02 $\gamma/s/b$
$\partial^2 L/\partial\sigma_2^2$	2.64718E-01 $\gamma/s/b^2$
$\partial^2 L/\partial\sigma_1\partial\sigma_2$	4.16462E+00 $\gamma/s/b^2$

TABLE V

Derivatives of the Leakage with Respect to Source Emission Rates

Parameter	Value
$\partial L/\partial q_1$	8.00043E-01 $\gamma/s/[\gamma/(10^{24} \text{ atoms}\cdot\text{s})]$
$\partial^2 L/\partial q_1^2$	0 $\gamma/s/[\gamma/(10^{24} \text{ atoms}\cdot\text{s})]^2$
$\partial L/\partial q_2$	0 $\gamma/s/[\gamma/(10^{24} \text{ atoms}\cdot\text{s})]$
$\partial^2 L/\partial q_2^2$	0 $\gamma/s/[\gamma/(10^{24} \text{ atoms}\cdot\text{s})]^2$
$\partial^2 L/\partial q_1\partial q_2$	0 $\gamma/s/[\gamma/(10^{24} \text{ atoms}\cdot\text{s})]^2$

TABLE VI

Derivatives of the Leakage with Respect to Material Density

Parameter	Value
$\partial L/\partial\rho$	1.08011E+02 $\gamma/s/(g/cm^3)$
$\partial^2 L/\partial\rho^2$	-2.05068E+01 $\gamma/s/(g/cm^3)^2$

of the 1st-LASS [i.e., Eqs. (1), (2), (28), and (29), which coincide for the linear transport equation with the usual forward and adjoint transport equations]. PARTISN is unable to accept angular fluxes as volumetric sources—only moments expansions are accepted.⁸ However, when anisotropic source moments are input, an anisotropic scattering expansion of (at least) the order of the source expansion is required. Thus, to use PARTISN on this problem requires inputting anisotropic scattering cross sections where no scattering is desired. (PARTISN allows negative sources and handles negative fluxes correctly if the negative flux fix-up is turned off.¹²)

To solve this problem, we used an L 'th-order scattering expansion and set the isotropic (0'th-order) scattering cross section and the L 'th-order scattering cross section to

TABLE VII

Mixed Derivatives of the Leakage*

Parameter	Value
$\partial^2 L/\partial N_1\partial\sigma_1$	-8.30901E+03 $\gamma/s/cm^{-1}$
$\partial^2 L/\partial N_1\partial\sigma_2$	2.67044E+03 $\gamma/s/cm^{-1}$
$\partial^2 L/\partial N_2\partial\sigma_1$	9.23334E+04 $\gamma/s/cm^{-1}$
$\partial^2 L/\partial N_2\partial\sigma_2$	-4.44522E+04 $\gamma/s/cm^{-1}$
$\partial^2 L/\partial N_1\partial q_1$	1.59779E+00 $\gamma/s/[\gamma/(cm^3\cdot s)]$
$\partial^2 L/\partial N_2\partial q_1$	-1.97856E+01 $\gamma/s/[\gamma/(cm^3\cdot s)]$
$\partial^2 L/\partial\sigma_1\partial q_1$	-1.40397E-02 $\gamma/s/[b\cdot\gamma/(10^{24} \text{ atoms}\cdot\text{s})]^2$
$\partial^2 L/\partial\sigma_2\partial q_1$	-8.92413E-04 $\gamma/s/[b\cdot\gamma/(10^{24} \text{ atoms}\cdot\text{s})]^2$
$\partial^2 L/\partial\rho\partial N_1$	-1.88165E+04 $\gamma/s/[(g/cm^3)(\text{atoms}/\{b\cdot\text{cm}\})]$
$\partial^2 L/\partial\rho\partial N_2$	1.59785E+05 $\gamma/s/[(g/cm^3)(\text{atoms}/\{b\cdot\text{cm}\})]$
$\partial^2 L/\partial\rho\partial\sigma_1$	-5.77782E+00 $\gamma/s/[g/(cm^3\cdot b)]$
$\partial^2 L/\partial\rho\partial\sigma_2$	-3.67258E-01 $\gamma/s/[g/(cm^3\cdot b)]$
$\partial^2 L/\partial\rho\partial q_1$	8.05453E-04 $\gamma/s/[g\cdot\gamma/cm^3/(10^{24} \text{ atoms}\cdot\text{s})]$

*All derivatives with respect to q_2 are zero.

10^{-24} times the total cross section. We set all other scattering cross-section moments to zero.

The MCCLIB04 cross sections were entered in the PARTISN input file using the ODNINP format.⁸ A mesh spacing of 0.005 cm was used (759 meshes in 3.794 cm).

The results presented in this section used a P_{31} scattering expansion and S_{2048} angular quadrature. With this quadrature order, the ratio of the leakage computed in the forward and adjoint calculations in the 1st-LASS was 1.00000270.

The difference between PARTISN results and analytic results for the leakage and derivatives of the mass density are shown in Table VIII. Density derivatives are obtained from PARTISN results using the chain rule:

$$\begin{aligned} \frac{\partial L}{\partial\rho} &= \sum_{i=1}^2 \frac{\partial L}{\partial N_i} \frac{\partial N_i}{\partial\rho} \\ &= \frac{N_1}{\rho} \frac{\partial L}{\partial N_1} + \frac{N_2}{\rho} \frac{\partial L}{\partial N_2} \end{aligned} \quad (110)$$

TABLE VIII

Difference Between Adjoint and Analytic Results for the Leakage and Mass Density Derivatives

Quantity	Difference
L	0.000%
$\partial L/\partial\rho$	-0.002%
$\partial^2 L/\partial\rho^2$	-0.002%

and

$$\begin{aligned} \frac{\partial^2 L}{\partial \rho^2} &= \sum_{i=1}^2 \sum_{j=1}^2 \frac{\partial^2 L}{\partial N_i \partial N_j} \frac{\partial N_i}{\partial \rho} \frac{\partial N_j}{\partial \rho} \\ &= \left(\frac{N_1}{\rho}\right)^2 \frac{\partial^2 L}{\partial N_1^2} + 2 \frac{N_1 N_2}{\rho} \frac{\partial^2 L}{\partial N_1 \partial N_2} + \left(\frac{N_2}{\rho}\right)^2 \frac{\partial^2 L}{\partial N_2^2}. \end{aligned} \tag{111}$$

These density derivatives are constant-volume partial derivatives.⁹ Mixed derivatives involving the mass density are obtained similarly.

The difference between PARTISN results and analytic results for isotopic first derivatives are shown in Table IX.

The difference between PARTISN results and analytic results for isotopic second derivatives (including mixed derivatives) are shown in Table X.

The difference between PARTISN results and analytic results for isotopic mixed second derivatives that include the mass density are shown in Table XI. Again, these are obtained from the PARTISN results using the chain rule [Eq. (A.30)], where α represents the isotopic density, cross section, or source emission rate for either isotope.

When a P_3 scattering expansion was used (still with an S_{2048} angular quadrature), errors in the isotopic second derivatives were up to 3%, except for $\partial^2 L / \partial q_1 \partial N_j$ and $\partial^2 L / \partial q_1 \partial \sigma_j$, which were still basically zero because the 2nd-LASS equations for those derivatives use only the physical source emission rate density, which is isotropic. Errors in the derivatives that include the mass density were larger, up to 7%.

TABLE IX

Difference Between Adjoint and Analytic Results for Isotopic First Derivatives

i	$\partial L / \partial N_i$
1 (²³⁹ Pu)	0.000%
2 (²⁴⁰ Pu)	0.000%
i	$\partial L / \partial \sigma_i$
1 (²³⁹ Pu)	0.000%
2 (²⁴⁰ Pu)	0.000%
i	$\partial L / \partial q_i$
1 (²³⁹ Pu)	0.000%
2 (²⁴⁰ Pu)	N/A ^a

^aNot applicable as all derivatives with respect to q_2 are zero.

Using many scattering moments was crucial to having PARTISN solve this problem correctly, but the choice of the scattering cross section is not important as long as it is very small. The first-order relative sensitivities of the leakage to the 0'th- and L 'th-order ²³⁹Pu scattering cross sections is 7E-25%/ and 5E-31%/ , respectively, and the sensitivities to the ²⁴⁰Pu scattering cross sections are an order of magnitude smaller.

V.E. Impact of Second-Order Sensitivities on Response Expected Value, Variance, and Skewness

In a second-order analysis, the expected value of a response R is²

$$E(R) = R(\alpha^0) + \frac{1}{2} \sum_{i=1}^{N_\alpha} \frac{\partial^2 R}{\partial \alpha_i^2} s_i^2, \tag{112}$$

where s_i is the standard deviation of input parameter α_i . The variance of response R is

$$\text{var}(R) = \sum_{i=1}^{N_\alpha} \left(\frac{\partial R}{\partial \alpha_i}\right)^2 s_i^2 + \frac{1}{2} \sum_{i=1}^{N_\alpha} \left(\frac{\partial^2 R}{\partial \alpha_i^2}\right)^2 s_i^4. \tag{113}$$

The skewness γ_1 of response R is

$$\gamma_1(R) = \frac{\mu_3(R)}{[\text{var}(R)]^{3/2}}, \tag{114}$$

where the third central moment $\mu_3(R)$ is

$$\mu_3(R) = 3 \sum_{i=1}^{N_\alpha} \left(\frac{\partial R}{\partial \alpha_i}\right)^2 \frac{\partial^2 R}{\partial \alpha_i^2} s_i^4. \tag{115}$$

Knowledge of the second-order sensitivities is required to compute these quantities.

To illustrate the importance of these calculations, various relative standard deviations were assumed for the atom densities of ²³⁹Pu and ²⁴⁰Pu, the plutonium cross section, and the source emission rate of the 646-keV line. All of these parameters were assumed to have (simultaneously) relative standard deviations of 1%, 5%, or 10%. [The ²³⁹Pu and ²⁴⁰Pu cross sections σ_1 and σ_2 are perfectly correlated. They are identical and their uncertainties are identical. To account for this correlation, Eq. (101) is replaced with $\Sigma = \sigma_1(N_1 + N_2)$ before the derivatives are computed.] The individual parameter contribution to the variance and skewness of the distribution of the total leakage, as well as the relative contribution of the second

TABLE X
Difference Between Adjoint and Analytic Results for Isotopic Second Derivatives

<i>i</i>	<i>j</i>	$\partial^2 L / \partial N_i \partial N_j$	$\partial^2 L / \partial N_i \partial \sigma_j$	$\partial^2 L / \partial N_i \partial q_j$
1 (²³⁹ Pu)	1 (²³⁹ Pu)	-0.001%	-0.002%	-0.002%
	2 (²⁴⁰ Pu)	0.000%	0.000%	N/A ^a
2 (²⁴⁰ Pu)	1 (²³⁹ Pu)	0.000%	0.000%	0.000%
	2 (²⁴⁰ Pu)	0.000%	0.000%	N/A ^a
<i>i</i>	<i>j</i>	$\partial^2 L / \partial \sigma_i \partial N_j$	$\partial^2 L / \partial \sigma_i \partial \sigma_j$	$\partial^2 L / \partial \sigma_i \partial q_j$
1 (²³⁹ Pu)	1 (²³⁹ Pu)	-0.001%	0.000%	0.000%
	2 (²⁴⁰ Pu)	0.000%	0.000%	N/A ^a
2 (²⁴⁰ Pu)	1 (²³⁹ Pu)	0.000%	0.000%	0.000%
	2 (²⁴⁰ Pu)	0.000%	0.000%	N/A ^a
<i>i</i>	<i>j</i>	$\partial^2 L / \partial q_i \partial N_j$	$\partial^2 L / \partial q_i \partial \sigma_j$	$\partial^2 L / \partial q_i \partial q_j$
1 (²³⁹ Pu)	1 (²³⁹ Pu)	0.000%	0.000%	N/A ^a
	2 (²⁴⁰ Pu)	0.000%	0.000%	N/A ^a
2 (²⁴⁰ Pu)	1 (²³⁹ Pu)	N/A ^a	N/A ^a	N/A ^a
	2 (²⁴⁰ Pu)	N/A ^a	N/A ^a	N/A ^a

^aNot applicable as all derivatives with respect to q_2 are zero.

TABLE XI

Difference Between Adjoint and Analytic Results for Mixed Second Derivatives that Include Mass Density

<i>j</i>	$\partial^2 L / \partial \rho \partial N_j$	$\partial^2 L / \partial \rho \partial \sigma_j$	$\partial^2 L / \partial \rho \partial q_j$
1 (²³⁹ Pu)	-0.001%	-0.002%	-0.002%
2 (²⁴⁰ Pu)	0.000%	-0.002%	N/A ^a

^aNot applicable as all derivatives with respect to q_2 are zero.

term to the total variance and expected value, are shown in Table XII. The combined values due to all uncertain parameters are given as the Total in the last three rows.

As expected,² the second-order sensitivities cause the expected value of the response to differ from the computed nominal value; they contribute somewhat to the overall variance; and most importantly, they constitute the only contribution to the asymmetry of the response distribution (skewness).

VI. CYLINDRICAL TEST PROBLEM

A two-dimensional (2-D) (*r-z*) cylindrical test problem is described in Sec. VI.A. Derivatives computed by solving the 1st- and 2nd-LASS using PARTISN are compared with values estimated using central differences in Sec. VI.B. Sensitivities given in Secs. IV.A, IV.B, and IV.C were

computed and are presented in this section; sensitivities to the detector parameters (Sec. IV.D) were not computed.

VI.A. Problem Setup

The geometry corresponds to a measurement that was performed at Oak Ridge National Laboratory.¹³ A polyethylene bottle containing depleted uranium (DU) in nitric acid solution was shielded by an aluminum disk from a high-purity germanium gamma-ray detector aimed at the bottom of the bottle. The quantity of interest in Ref. 13 was the uncollided flux or photopeak count rate in the detector of the various lines emitted from uranium. The quantity of interest in the present application is the total uncollided leakage rate of the 1.001-MeV line from the entire system pictured in Fig. 1. The materials in the model are specified in Table XIII.

The polyethylene bottle is modeled with outer radius 2.4 cm, radial wall thickness 0.1 cm, outside height 6.6 cm, and top and bottom wall thicknesses 0.2 cm. The height of the solution above the bottle is 4.0 cm. The radius and thickness of the aluminum shield are 4.0 and 1.0 cm, respectively. Unfilled regions on Fig. 1 are voids.

The cross sections were obtained from the MCPLIB04 ACE-formatted photon cross-section library and do not contain coherent scattering. The source emission rate for the 1.001-MeV line is 4.033E+04 $\gamma/(10^{24}$ atoms ²³⁸U)/s

TABLE XII
Variance, Skewness, and Expected Value of the Leakage for the Analytic Sphere

	Relative Standard Deviation	var(L) ^a	Contribution of Second Term to var(L) ^a	Skewness ^b	Contribution of Second Term to E(L) ^c
N ₁	1%	6.42773E+03	0.021%	-6.13217E-02	-0.001%
	5%	1.61499E+05	0.520%	-3.04316E-01	-0.019%
	10%	6.56072E+05	2.048%	-5.94666E-01	-0.076%
N ₂	1%	3.98148E+03	0.000%	3.49894E-03	0.000%
	5%	9.95387E+04	0.002%	1.74943E-02	0.001%
	10%	3.98175E+05	0.007%	3.49858E-02	0.003%
σ ₁	1%	1.11491E+06	0.019%	5.85286E-02	0.010%
	5%	2.80001E+07	0.474%	2.90649E-01	0.240%
	10%	1.13592E+08	1.869%	5.69121E-01	0.960%
q ₁	1%	1.15102E+06	0.000%	0.00000E+00	0.000%
	5%	2.87756E+07	0.000%	0.00000E+00	0.000%
	10%	1.15102E+08	0.000%	0.00000E+00	0.000%
Total	1%	2.27634E+06	0.009%	2.00529E-02	0.009%
	5%	5.70367E+07	0.234%	9.99268E-02	0.222%
	10%	2.29749E+08	0.930%	1.97767E-01	0.887%

^aEquation (113).
^bEquation (114).
^cEquation (112).

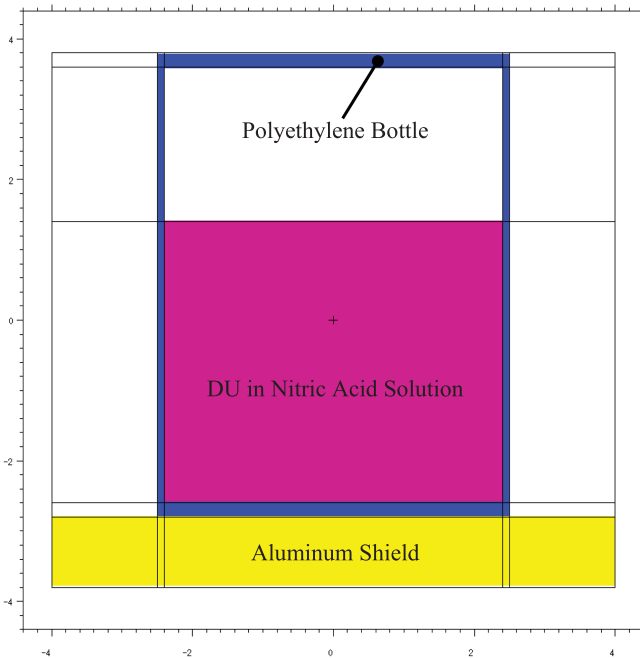


Fig. 1. Cross-section (r-z) of the cylindrical geometry. (Scales in centimeters.)

from Gunnick and Tinney.¹⁴ (The line is actually from ^{234m}Pa, a daughter of ²³⁸U in secular equilibrium with it.)

The PARTISN calculations used S₁₂₈ square Chebyshev-Legendre angular quadrature. They also used

a P₃₁ Legendre scattering expansion as discussed in Sec. V.D. With these parameters, the ratio of the leakage computed in the forward and adjoint calculations in the 1st-LASS was 1.00000355. The total uncollided leakage was 62.034780/s.

The detector response function for this problem is Eq. (109).

VI.B. Results

Counting ¹H once for each material in which it appears, there are seven isotopes in this problem (Table XIII). Counting three material mass densities, the atom density, and total cross section for each isotope, and one source emission rate, this problem has 18 first-order sensitivities and 224 second-order sensitivities to compare. (Second derivatives of the mass density are included, but mixed partial derivatives that include the mass density are not.)

The results obtained using the 1st- and 2nd-LASS formulas presented in Sec. IV were compared with central-difference sensitivity estimates for each of the 242 sensitivities. There were 877 PARTISN calculations needed (including the base-case forward calculation) to compute the central differences, and this number does not include the additional calculations that were required to find appropriate values of the perturbations to use for the

TABLE XIII
Materials in the Cylindrical Test Problem

Index	Material	Composition (Weight Fraction)	Density (g/cm ³)
1	DU in Nitric Acid	²³⁵ U 0.000033959; ²³⁸ U 0.00996604; ¹⁶ O 0.883106; ¹ H 0.106894	1.025 ^a
2	Polyethylene	¹ H 0.143716; C 0.856284	0.93
3	Aluminum	²⁷ Al 1	2.7

^aIncorrectly given as 0.998 g/cm³ in Ref. 13.

central differences. The 1st- and 2nd-LASS formulas required just 12 PARTISN calculations.

Table XIV presents results for a small subset of the computed sensitivities: the second derivatives involving ²³⁸U (isotope 2). The agreement is generally within 0.3%, except for $\partial^2 L / \partial \sigma_2 \partial N_1$ and $\partial^2 L / \partial \sigma_2 \partial \sigma_1$, for which the difference is -29%. The central differences for these derivatives are extremely difficult to calculate: Changing the ²³⁸U cross section by ±90% and the ²³⁵U density and cross section by ±99% yielded changes of only 0.12%

(in magnitude) in the total leakage rate. In Table XIV, the derivatives computed using the 2nd-LASS are more accurate than those computed by central differences.

VI.C. Impact of Second-Order Sensitivities on Response Expected Value, Variance, and Skewness

The mass densities of the three materials were assumed to have (simultaneously) relative standard deviations of 1%, 5%, or 10%. The individual parameter

TABLE XIV
Difference Between Adjoint and Central Differences for Isotopic Second Derivatives Involving ²³⁸U

<i>j</i>	$\partial^2 L / \partial N_2 \partial N_j$	$\partial^2 L / \partial N_2 \partial \sigma_j$	$\partial^2 L / \partial N_2 \partial q_j$
1 (²³⁵ U)	-0.296%	-0.296%	N/A ^a
2 (²³⁸ U)	0.020%	0.005%	0.000%
3 (¹⁶ O)	0.000%	0.000%	N/A ^a
4 (¹ H) ^(b)	0.001%	0.001%	N/A ^a
5 (¹ H) ^(b)	-0.001%	-0.001%	N/A ^a
6 (C)	0.005%	0.005%	N/A ^a
7 (²⁷ Al)	-0.003%	-0.003%	N/A ^a
<i>j</i>	$\partial^2 L / \partial \sigma_2 \partial N_j$	$\partial^2 L / \partial \sigma_2 \partial \sigma_j$	$\partial^2 L / \partial \sigma_2 \partial q_j$
1 (²³⁵ U)	-28.6%	-28.6%	N/A ^a
2 (²³⁸ U)	0.006%	-0.547%	-0.024%
3 (¹⁶ O)	-0.079%	-0.079%	N/A ^a
4 (¹ H) ^b	0.271%	0.271%	N/A ^a
5 (¹ H) ^b	-0.269%	-0.269%	N/A ^a
6 (C)	-0.264%	-0.264%	N/A ^a
7 (²⁷ Al)	-0.058%	-0.058%	N/A ^a
<i>j</i>	$\partial^2 L / \partial q_2 \partial N_j$	$\partial^2 L / \partial q_2 \partial \sigma_j$	$\partial^2 L / \partial q_2 \partial q_j$
1 (²³⁵ U)	-0.090%	-0.090%	N/A ^a
2 (²³⁸ U)	0.000%	-0.025%	N/A ^c
3 (¹⁶ O)	0.000%	0.000%	N/A ^a
4 (¹ H) ^b	0.000%	0.000%	N/A ^a
5 (¹ H) ^b	0.005%	0.005%	N/A ^a
6 (C)	0.000%	0.001%	N/A ^a
7 (²⁷ Al)	-0.001%	-0.001%	N/A ^a

^aNot applicable as all derivatives with respect to *q_j* are zero for *j* ≠ 2.

^bIsotope 4 is ¹H in the nitric acid solution. Isotope 5 is ¹H in polyethylene.

^cNot applicable: $\partial^2 L / \partial q_2^2 = 0$.

contribution to the variance and skewness of the distribution of the total leakage, as well as the relative contribution of the second term to the total variance and expected value, are shown in Table XV. The combined values due to all uncertain parameters are given as the Total in the last three rows. Here the second-order effects on the expected value of the response and the variance are minimal, but the second-order effects constitute the only contribution to the asymmetry of the response distribution (skewness).

VII. SPHERICAL TEST PROBLEM (NONANALYTIC)

A two-region one-dimensional spherical test problem is described in Sec. VII.A. Derivatives computed by solving the 1st- and 2nd-LASS using PARTISN are compared with values estimated using central differences in Sec. VII.B. Sensitivities given in Secs. IV.A through IV.D were computed and are presented in this section.

VII.A. Problem Setup

The problem is a simplified version of the Beryllium-Reflected Plutonium (BeRP) ball^{15,16} reflected by 3.81 cm of polyethylene. The materials are specified in Table XVI. The radius of the inner sphere containing α -phase plutonium was $r_1 = 3.794$ cm and the radius of the outer shell containing polyethylene was $r_2 = 7.604$ cm.

The quantity of interest R was the total reaction rate of the 646-keV gamma-ray line from ²³⁹Pu in the carbon of the polyethylene shell. Thus the response function used in Eq. (3) was

$$\Sigma_d(\mathbf{r}, \boldsymbol{\Omega}) = \begin{cases} 0, & 0 \leq r < r_1 \\ N_C \sigma_C, & r_1 \leq r \leq r_2, \end{cases} \quad (116)$$

where N_C and σ_C are the atom density of carbon in the material and the microscopic total cross section of carbon at 646 keV. Also, λ_k of Eq. (35) is $\Sigma_C = N_C \sigma_C$. Recall from Secs. II, III, and IV that the sensitivities of R to the

TABLE XV
Variance, Skewness, and Expected Value of the Leakage for the Cylinder

	Relative Standard Deviation	var(L) ^a	Contribution of Second Term to var(L) ^a	Skewness ^b	Contribution of Second Term to E(L) ^c
ρ_1	1%	2.92283E-01	0.000%	-7.99062E-03	-0.001%
	5%	7.30769E+00	0.009%	-3.99480E-02	-0.029%
	10%	2.92386E+01	0.035%	-7.98641E-02	-0.116%
ρ_2	1%	6.07983E-05	0.000%	5.51151E-04	0.000%
	5%	1.51996E-03	0.000%	2.75575E-03	0.000%
	10%	6.07984E-03	0.000%	5.51149E-03	0.000%
ρ_3	1%	7.90354E-04	0.000%	7.31610E-03	0.000%
	5%	1.97603E-02	0.007%	3.65766E-02	0.001%
	10%	7.90587E-02	0.030%	7.31287E-02	0.006%
Total	1%	2.93134E-01	0.000%	-7.95482E-03	-0.001%
	5%	7.32898E+00	0.009%	-3.97690E-02	-0.028%
	10%	2.93237E+01	0.035%	-7.95063E-02	-0.110%

^aEquation (113).
^bEquation (114).
^cEquation (112).

TABLE XVI
Materials in the Simplified BeRP Ball

Index	Material	Composition (Weight Fraction)	Density (g/cm ³)
1	α -phase plutonium	²³⁹ Pu 0.938039; ²⁴⁰ Pu 0.0594113; ⁶⁹ Ga 0.00151516; ⁷⁰ Ga 0.00103465	19.6
2	Polyethylene	C 0.856299; ¹ H 0.143701	0.95

detector response function assume that perturbations in the detector response function do not affect the gamma-ray flux. Therefore, changing the polyethylene density or composition does not change the response function.

VII.B. Results

The reaction rate $R = 2.574052 \times 10^4/s$. The first and second derivatives of R with respect to the mass densities of the materials are shown in Table XVII. These quantities were calculated using the 1st- and 2nd-LASS equations as well least-squares fits from the second-order polynomials shown in Fig. 2. The fits were used because the second derivatives are small and extremely difficult to calculate using a finite difference. A more accurate and efficient direct method could be used, but the point here is that the 2nd-LASS gives the second-order sensitivities efficiently and exactly without the difficulties associated with finite differences.

The mixed partial derivatives $\partial^2 R / \partial \Sigma_C \partial N_i$ are compared with finite differences in Table XVIII. The agreement is excellent, but only after significant effort was

expended in trial-and-error to determine appropriate values to perturb the response function and the atom densities for the finite differences. (The final perturbation amounts are shown on Table XVIII.) Again, this effort is avoided when the 2nd-LASS is used.

VII.C. Impact of Second-Order Sensitivities on Response Expected Value, Variance, and Skewness

The microscopic cross sections of the six isotopes were assumed to have (simultaneously) a relative standard deviation of 1%. Because the ^{239}Pu and ^{240}Pu cross sections are perfectly correlated and the ^{69}Ga and ^{71}Ga cross sections are perfectly correlated, the sums of the first derivatives and the sums of the second derivatives for the isotopes were used. The individual parameter contribution to the variance and skewness of the distribution of the total leakage, as well as the relative contribution of the second term to the total variance and expected value, are shown in Table XIX. The combined values due to all uncertain parameters are given as the

TABLE XVII
Derivatives of the Reaction Rate with Respect to Mass Densities

Derivative	Fit	Adjoint	Difference
$\partial R / \partial \rho_{\text{Pu}}$	1.70204E+01	1.69813E+01	-0.230%
$\partial R / \partial \rho_{\text{Poly}}$	-4.94965E+03	-4.94952E+03	-0.003%
$\partial^2 R / \partial \rho_{\text{Pu}}^2$	-2.55237E+00	-2.54190E+00	-0.410%
$\partial^2 R / \partial \rho_{\text{Poly}}^2$	1.34067E+03	1.33640E+03	-0.319%

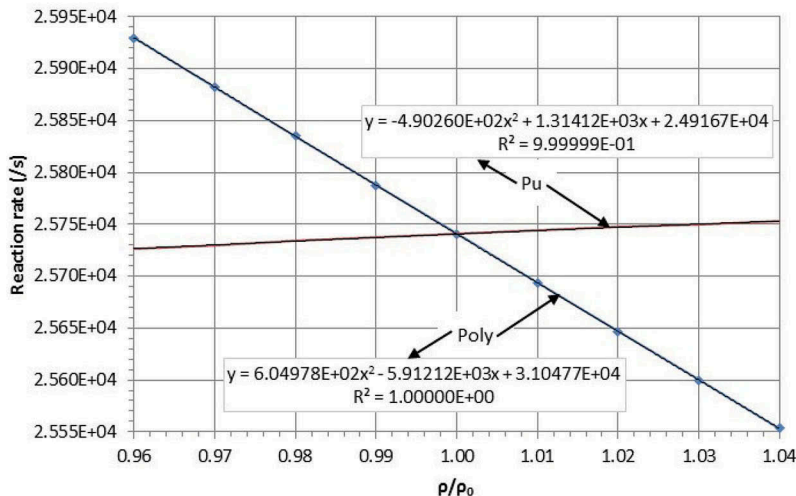


Fig. 2. Reaction rate as a function of (relative) material densities.

TABLE XVIII
Derivatives of the Reaction Rate with Respect to Σ_C and N_i

Index	Finite Difference	$p(\Sigma_C), p(N_i)$ (%)	Adjoint	Difference
1	6.38450E+05	15, 3	6.38610E+05	-0.025%
2	-8.13718E+06	10, 20	-8.13920E+06	-0.025%
3	-1.26141E+06	50, 90	-1.26178E+06	-0.029%
4	-1.26381E+06	50, 90	-1.26178E+06	0.161%
5	-1.36642E+06	3.5, 10	-1.36560E+06	0.060%
6	-2.27506E+05	5, 40	-2.27618E+05	-0.049%

TABLE XIX
Variance, Skewness, and Expected Value of the Reaction Rate for the Reflected BeRP Ball

Isotope	$\text{var}(R)^a$	Contribution of Second Term to $\text{var}(R)^a$	Skewness ^b	Contribution of Second Term to $E(R)^c$
$^{239}\text{Pu} + ^{240}\text{Pu}$	6.43896E+04	0.015%	5.21958E-02	0.009%
$^{69}\text{Ga} + ^{71}\text{Ga}$	1.18914E-01	0.000%	4.15670E-05	0.000%
^1H	1.24360E+03	0.000%	5.77124E-03	0.000%
C	1.38198E+02	0.000%	1.92389E-03	0.000%
Total	6.57715E+04	0.015%	5.05747E-02	0.009%

^aEquation (113).

^bEquation (114).

^cEquation (112).

Total in the last three rows. The second-order effects on the expected value of the response and the variance are minimal, but the second-order effects constitute the only contribution to the asymmetry of the response distribution (skewness).

Note that the second-order sensitivity of R to the detector response function contributes nothing to the quantities of Table XIX [Eq. (100)].

VIII. SUMMARY AND CONCLUSIONS

In this paper, Cacuci's 2nd-ASAM was applied to derive second-order sensitivities of a detector response to uncollided particles with respect to isotopic number densities, microscopic cross sections, source emission rates, and detector response parameters. These exact second-order sensitivities are computed using 2nd-LASS, which differ from the original forward Boltzmann equation and its adjoint only by the sources on the right sides of the 2nd-LASS equations. In the absence of the 2nd-ASAM, second-order sensitivities would need to be computed by many hundreds of recomputations in conjunction with

inexact finite-difference approximations. The equations of the 2nd-LASS were solved using the PARTISN discrete-ordinates code, and the solutions were subsequently used to compute second-order sensitivities for three test problems: a homogeneous spherical system, an inhomogeneous 2-D (r - z) cylindrical system, and a two-region sphere. The exact sensitivities computed using the 2nd-ASAM were compared with the values that would have been obtained by using finite differences.

The ability to use an off-the-shelf discrete-ordinates code, PARTISN, for the transport calculations indicates the general applicability of the 2nd-ASAM. It is easier if the chosen transport code can handle negative sources and negative fluxes, but the sources can always be split and the results subtracted as necessary.¹² But the paramount reason for applying the 2nd-ASAM is the significant reduction, by orders of magnitude, of the number of large-scale computations needed for obtaining the first- and second-order sensitivities of system responses to system parameters. Ongoing research aims at generalizing the 2nd-ASAM to enable the computation of arbitrarily high-order response sensitivities along with applications to large-scale problems.

APPENDIX

DERIVATIVES OF THE LEAKAGE FOR THE HOMOGENEOUS SPHERE

A.I. DERIVATIVES WITH RESPECT TO ATOM DENSITIES

The first derivative of the leakage with respect to N_1 is

$$\begin{aligned} \frac{\partial L}{\partial N_1} &= \frac{\partial Q}{\partial N_1} P + Q \frac{\partial P}{\partial N_1} \\ &= q_1 V P + Q \frac{\partial P}{\partial \Sigma} \frac{\partial \Sigma}{\partial N_1} \\ &= q_1 V P + Q \sigma_1 \frac{\partial P}{\partial \Sigma}. \end{aligned} \tag{A.1}$$

The first derivative of the leakage with respect to N_2 is

$$\begin{aligned} \frac{\partial L}{\partial N_2} &= \frac{\partial Q}{\partial N_2} P + Q \frac{\partial P}{\partial N_2} \\ &= Q \frac{\partial P}{\partial \Sigma} \frac{\partial \Sigma}{\partial N_2} \\ &= Q \sigma_2 \frac{\partial P}{\partial \Sigma}. \end{aligned} \tag{A.2}$$

The second derivative of the leakage with respect to N_1 is

$$\begin{aligned} \frac{\partial^2 L}{\partial N_1^2} &= q_1 V \frac{\partial P}{\partial N_1} + \frac{\partial Q}{\partial N_1} \sigma_1 \frac{\partial P}{\partial \Sigma} + Q \sigma_1 \frac{\partial}{\partial N_1} \left(\frac{\partial P}{\partial \Sigma} \right) \\ &= q_1 V \frac{\partial P}{\partial \Sigma} \frac{\partial \Sigma}{\partial N_1} + q_1 V \sigma_1 \frac{\partial P}{\partial \Sigma} + Q \sigma_1 \frac{\partial}{\partial \Sigma} \left(\frac{\partial P}{\partial \Sigma} \right) \frac{\partial \Sigma}{\partial N_1} \\ &= 2q_1 V \sigma_1 \frac{\partial P}{\partial \Sigma} + Q \sigma_1^2 \frac{\partial^2 P}{\partial \Sigma^2}. \end{aligned} \tag{A.3}$$

The second derivative of the leakage with respect to N_2 is

$$\begin{aligned} \frac{\partial^2 L}{\partial N_2^2} &= \frac{\partial Q}{\partial N_2} \sigma_2 \frac{\partial P}{\partial \Sigma} + Q \sigma_2 \frac{\partial}{\partial N_2} \left(\frac{\partial P}{\partial \Sigma} \right) \\ &= Q \sigma_2 \frac{\partial}{\partial \Sigma} \left(\frac{\partial P}{\partial \Sigma} \right) \frac{\partial \Sigma}{\partial N_2} \\ &= Q \sigma_2^2 \frac{\partial^2 P}{\partial \Sigma^2}. \end{aligned} \tag{A.4}$$

The mixed partial derivative of the leakage with respect to N_1 and N_2 , by differentiating Eq. (A.2) with respect to N_1 , is

$$\begin{aligned} \frac{\partial^2 L}{\partial N_1 \partial N_2} &= \frac{\partial Q}{\partial N_1} \sigma_2 \frac{\partial P}{\partial \Sigma} + Q \sigma_2 \frac{\partial}{\partial N_1} \left(\frac{\partial P}{\partial \Sigma} \right) \\ &= q_1 V \sigma_2 \frac{\partial P}{\partial \Sigma} + Q \sigma_2 \frac{\partial}{\partial \Sigma} \left(\frac{\partial P}{\partial \Sigma} \right) \frac{\partial \Sigma}{\partial N_1} \\ &= q_1 V \sigma_2 \frac{\partial P}{\partial \Sigma} + Q \sigma_1 \sigma_2 \frac{\partial^2 P}{\partial \Sigma^2}. \end{aligned} \tag{A.5}$$

Differentiating Eq. (A.1) with respect to N_2 also gives Eq. (A.5).

A.II. DERIVATIVES WITH RESPECT TO CROSS SECTIONS

The first derivative of the leakage with respect to σ_1 is

$$\begin{aligned} \frac{\partial L}{\partial \sigma_1} &= \frac{\partial Q}{\partial \sigma_1} P + Q \frac{\partial P}{\partial \sigma_1} \\ &= Q \frac{\partial P}{\partial \Sigma} \frac{\partial \Sigma}{\partial \sigma_1} \\ &= Q N_1 \frac{\partial P}{\partial \Sigma}. \end{aligned} \tag{A.6}$$

The first derivative of the leakage with respect to σ_2 is

$$\begin{aligned} \frac{\partial L}{\partial \sigma_2} &= \frac{\partial Q}{\partial \sigma_2} P + Q \frac{\partial P}{\partial \sigma_2} \\ &= Q \frac{\partial P}{\partial \Sigma} \frac{\partial \Sigma}{\partial \sigma_2} \\ &= Q N_2 \frac{\partial P}{\partial \Sigma}. \end{aligned} \tag{A.7}$$

The second derivative of the leakage with respect to σ_1 is

$$\begin{aligned} \frac{\partial^2 L}{\partial \sigma_1^2} &= \frac{\partial Q}{\partial \sigma_1} N_1 \frac{\partial P}{\partial \Sigma} + Q N_1 \frac{\partial}{\partial \sigma_1} \left(\frac{\partial P}{\partial \Sigma} \right) \\ &= Q N_1 \frac{\partial}{\partial \Sigma} \left(\frac{\partial P}{\partial \Sigma} \right) \frac{\partial \Sigma}{\partial \sigma_1} \\ &= Q N_1^2 \frac{\partial^2 P}{\partial \Sigma^2}. \end{aligned} \tag{A.8}$$

The second derivative of the leakage with respect to σ_2 is

$$\begin{aligned} \frac{\partial^2 L}{\partial \sigma_2^2} &= \frac{\partial Q}{\partial \sigma_2} N_2 \frac{\partial P}{\partial \Sigma} + Q N_2 \frac{\partial}{\partial \sigma_2} \left(\frac{\partial P}{\partial \Sigma} \right) \\ &= Q N_2 \frac{\partial}{\partial \Sigma} \left(\frac{\partial P}{\partial \Sigma} \right) \frac{\partial \Sigma}{\partial \sigma_2} \\ &= Q N_2^2 \frac{\partial^2 P}{\partial \Sigma^2} . \end{aligned} \quad (\text{A.9})$$

$$\Sigma = \frac{\rho}{\rho_0} \Sigma_0 \quad (\text{A.13})$$

and

$$Q = \frac{\rho}{\rho_0} Q_0 , \quad (\text{A.14})$$

The mixed partial derivative of the leakage with respect to σ_1 and σ_2 , by differentiating Eq. (A.7) with respect to σ_1 , is

$$\begin{aligned} \frac{\partial^2 L}{\partial \sigma_1 \partial \sigma_2} &= \frac{\partial Q}{\partial \sigma_1} N_2 \frac{\partial P}{\partial \Sigma} + Q N_2 \frac{\partial}{\partial \sigma_1} \left(\frac{\partial P}{\partial \Sigma} \right) \\ &= Q N_2 \frac{\partial}{\partial \Sigma} \left(\frac{\partial P}{\partial \Sigma} \right) \frac{\partial \Sigma}{\partial \sigma_1} \\ &= Q N_1 N_2 \frac{\partial^2 P}{\partial \Sigma^2} . \end{aligned} \quad (\text{A.10})$$

Differentiating Eq. (A.6) with respect to σ_2 also gives Eq. (A.10).

A.III. DERIVATIVES WITH RESPECT TO SOURCE EMISSION RATES

The first derivative of the leakage with respect to q_1 is

$$\begin{aligned} \frac{\partial L}{\partial q_1} &= \frac{\partial Q}{\partial q_1} P + Q \frac{\partial P}{\partial q_1} \\ &= N_1 V P . \end{aligned} \quad (\text{A.11})$$

The first derivative of the leakage with respect to q_2 is zero.

The second derivative of the leakage with respect to q_1 is

$$\frac{\partial^2 L}{\partial q_1^2} = N_1 V \frac{\partial P}{\partial q_1} = 0 . \quad (\text{A.12})$$

The second derivative of the leakage with respect to q_2 is zero.

The mixed partial derivative of the leakage with respect to q_1 and q_2 is zero.

A.IV. DERIVATIVES WITH RESPECT TO MATERIAL MASS DENSITY

The material mass density ρ is also a quantity of interest. Using Eq. (103) in Eqs. (1) and (105), the cross section and total source rate can be written as

respectively, where subscript 0 represents the initial, unperturbed configuration.

The first derivative of the leakage with respect to ρ is

$$\begin{aligned} \frac{\partial L}{\partial \rho} &= \frac{\partial Q}{\partial \rho} P + Q \frac{\partial P}{\partial \rho} \\ &= \frac{\partial Q}{\partial \rho} P + Q \frac{\partial P}{\partial \Sigma} \frac{\partial \Sigma}{\partial \rho} . \end{aligned} \quad (\text{A.15})$$

Using Eqs. (A.13) and (A.14) yields

$$\frac{\partial L}{\partial \rho} = \frac{Q_0}{\rho_0} P + Q \frac{\Sigma_0}{\rho_0} \frac{\partial P}{\partial \Sigma} . \quad (\text{A.16})$$

Rearranging Eqs. (A.13) and (A.14), Eq. (A.16) can be written in the notation of the rest of this paper:

$$\frac{\partial L}{\partial \rho} = \frac{Q}{\rho} \left(P + \Sigma \frac{\partial P}{\partial \Sigma} \right) . \quad (\text{A.17})$$

From Eq. (A.16), the second derivative of the leakage with respect to ρ is

$$\begin{aligned} \frac{\partial^2 L}{\partial \rho^2} &= \frac{Q_0}{\rho_0} \frac{\partial P}{\partial \rho} + \frac{\partial Q}{\partial \rho} \frac{\Sigma_0}{\rho_0} \frac{\partial P}{\partial \Sigma} + Q \frac{\Sigma_0}{\rho_0} \frac{\partial}{\partial \rho} \left(\frac{\partial P}{\partial \Sigma} \right) \\ &= \frac{Q_0}{\rho_0} \frac{\partial P}{\partial \Sigma} \frac{\partial \Sigma}{\partial \rho} + \frac{\partial Q}{\partial \rho} \frac{\Sigma_0}{\rho_0} \frac{\partial P}{\partial \Sigma} + Q \frac{\Sigma_0}{\rho_0} \frac{\partial}{\partial \Sigma} \left(\frac{\partial P}{\partial \Sigma} \right) \frac{\partial \Sigma}{\partial \rho} \\ &= 2 \frac{Q_0}{\rho_0} \frac{\Sigma_0}{\rho_0} \frac{\partial P}{\partial \Sigma} + Q \left(\frac{\Sigma_0}{\rho_0} \right)^2 \frac{\partial^2 P}{\partial \Sigma^2} . \end{aligned} \quad (\text{A.18})$$

Again, rearranging Eqs. (A.13) and (A.14), Eq. (A.18) can be written in the notation of the rest of this paper:

$$\begin{aligned} \frac{\partial^2 L}{\partial \rho^2} &= 2 \frac{Q}{\rho} \frac{\partial P}{\partial \Sigma} + Q \left(\frac{\Sigma}{\rho} \right)^2 \frac{\partial^2 P}{\partial \Sigma^2} \\ &= \frac{Q}{\rho^2} \left(2 \Sigma \frac{\partial P}{\partial \Sigma} + \Sigma^2 \frac{\partial^2 P}{\partial \Sigma^2} \right) . \end{aligned} \quad (\text{A.19})$$

These density derivatives are constant-volume partial derivatives.⁹

A.V. MIXED DERIVATIVES: ATOM DENSITIES AND CROSS SECTIONS

The mixed partial derivative of the leakage with respect to N_1 and σ_1 , by differentiating Eq. (A.6) with respect to N_1 , is

$$\begin{aligned}\frac{\partial^2 L}{\partial N_1 \partial \sigma_1} &= \frac{\partial Q}{\partial N_1} N_1 \frac{\partial P}{\partial \Sigma} + Q \frac{\partial P}{\partial \Sigma} + Q N_1 \frac{\partial}{\partial N_1} \left(\frac{\partial P}{\partial \Sigma} \right) \\ &= q_1 V N_1 \frac{\partial P}{\partial \Sigma} + Q \frac{\partial P}{\partial \Sigma} + Q N_1 \frac{\partial}{\partial \Sigma} \left(\frac{\partial P}{\partial \Sigma} \right) \frac{\partial \Sigma}{\partial N_1} \\ &= 2Q \frac{\partial P}{\partial \Sigma} + Q N_1 \sigma_1 \frac{\partial^2 P}{\partial \Sigma^2}.\end{aligned}\quad (\text{A.20})$$

The mixed partial derivative of the leakage with respect to N_1 and σ_2 , by differentiating Eq. (A.7) with respect to N_1 , is

$$\begin{aligned}\frac{\partial^2 L}{\partial N_1 \partial \sigma_2} &= \frac{\partial Q}{\partial N_1} N_2 \frac{\partial P}{\partial \Sigma} + Q N_2 \frac{\partial}{\partial N_1} \left(\frac{\partial P}{\partial \Sigma} \right) \\ &= q_1 V N_2 \frac{\partial P}{\partial \Sigma} + Q N_2 \frac{\partial}{\partial \Sigma} \left(\frac{\partial P}{\partial \Sigma} \right) \frac{\partial \Sigma}{\partial N_1} \\ &= q_1 V N_2 \frac{\partial P}{\partial \Sigma} + Q N_2 \sigma_1 \frac{\partial^2 P}{\partial \Sigma^2}.\end{aligned}\quad (\text{A.21})$$

Differentiating Eq. (A.1) with respect to σ_1 and (separately) σ_2 also gives Eqs. (A.20) and (A.21).

The mixed partial derivative of the leakage with respect to N_2 and σ_1 , by differentiating Eq. (A.6) with respect to N_2 , is

$$\begin{aligned}\frac{\partial^2 L}{\partial N_2 \partial \sigma_1} &= \frac{\partial Q}{\partial N_2} N_1 \frac{\partial P}{\partial \Sigma} + Q N_1 \frac{\partial}{\partial N_2} \left(\frac{\partial P}{\partial \Sigma} \right) \\ &= Q N_1 \frac{\partial}{\partial \Sigma} \left(\frac{\partial P}{\partial \Sigma} \right) \frac{\partial \Sigma}{\partial N_2} \\ &= Q N_1 \sigma_2 \frac{\partial^2 P}{\partial \Sigma^2}.\end{aligned}\quad (\text{A.22})$$

The mixed partial derivative of the leakage with respect to N_2 and σ_2 , by differentiating Eq. (A.7) with respect to N_2 , is

$$\begin{aligned}\frac{\partial^2 L}{\partial N_2 \partial \sigma_2} &= \frac{\partial Q}{\partial N_2} N_2 \frac{\partial P}{\partial \Sigma} + Q \frac{\partial P}{\partial \Sigma} + Q N_2 \frac{\partial}{\partial N_2} \left(\frac{\partial P}{\partial \Sigma} \right) \\ &= Q \frac{\partial P}{\partial \Sigma} + Q N_2 \frac{\partial}{\partial \Sigma} \left(\frac{\partial P}{\partial \Sigma} \right) \frac{\partial \Sigma}{\partial N_2} \\ &= Q \frac{\partial P}{\partial \Sigma} + Q N_2 \sigma_2 \frac{\partial^2 P}{\partial \Sigma^2}.\end{aligned}\quad (\text{A.23})$$

Differentiating Eq. (A.2) with respect to σ_1 and (separately) σ_2 also gives Eqs. (A.22) and (A.23).

These density derivatives are constant-volume partial derivatives.⁹

A.VI. MIXED DERIVATIVES: ATOM DENSITIES AND SOURCE EMISSION RATES

The mixed partial derivative of the leakage with respect to N_1 and q_1 , by differentiating Eq. (A.11) with respect to N_1 , is

$$\begin{aligned}\frac{\partial^2 L}{\partial N_1 \partial q_1} &= V P + N_1 V \frac{\partial P}{\partial N_1} \\ &= V P + N_1 V \frac{\partial P}{\partial \Sigma} \frac{\partial \Sigma}{\partial N_1} \\ &= V P + N_1 V \sigma_1 \frac{\partial P}{\partial \Sigma}.\end{aligned}\quad (\text{A.24})$$

The mixed partial derivative of the leakage with respect to N_1 and q_2 is zero. Differentiating Eq. (A.1) with respect to q_1 also gives Eq. (A.24).

The mixed partial derivative of the leakage with respect to N_2 and q_1 , by differentiating Eq. (A.11) with respect to N_2 , is

$$\begin{aligned}\frac{\partial^2 L}{\partial N_2 \partial q_1} &= N_1 V \frac{\partial P}{\partial N_2} \\ &= N_1 V \frac{\partial P}{\partial \Sigma} \frac{\partial \Sigma}{\partial N_2} \\ &= N_1 V \sigma_2 \frac{\partial P}{\partial \Sigma}.\end{aligned}\quad (\text{A.25})$$

The mixed partial derivative of the leakage with respect to N_2 and q_2 is zero. Differentiating Eq. (A.2) with respect to q_1 also gives Eq. (A.25).

These density derivatives are constant-volume partial derivatives.⁹

A.VII. MIXED DERIVATIVES: CROSS SECTIONS AND SOURCE EMISSION RATES

The mixed partial derivative of the leakage with respect to σ_1 and q_1 , by differentiating Eq. (A.11) with respect to σ_1 , is

$$\begin{aligned}\frac{\partial^2 L}{\partial \sigma_1 \partial q_1} &= N_1 V \frac{\partial P}{\partial \sigma_1} \\ &= N_1 V \frac{\partial P}{\partial \Sigma} \frac{\partial \Sigma}{\partial \sigma_1} \\ &= N_1^2 V \frac{\partial P}{\partial \Sigma}.\end{aligned}\quad (\text{A.26})$$

The mixed partial derivative of the leakage with respect to σ_1 and q_2 is zero. Differentiating Eq. (A.6) with respect to q_1 also gives Eq. (A.26).

The mixed partial derivative of the leakage with respect to σ_2 and q_1 , by differentiating Eq. (A.11) with respect to σ_2 , is

$$\begin{aligned} \frac{\partial^2 L}{\partial \sigma_2 \partial q_1} &= N_1 V \frac{\partial P}{\partial \sigma_2} \\ &= N_1 V \frac{\partial P}{\partial \Sigma} \frac{\partial \Sigma}{\partial \sigma_2} \\ &= N_1 N_2 V \frac{\partial P}{\partial \Sigma}. \end{aligned} \quad (\text{A.27})$$

The mixed partial derivative of the leakage with respect to σ_2 and q_2 is zero. Differentiating Eq. (A.7) with respect to q_1 also gives Eq. (A.27).

A.VIII. MIXED DERIVATIVES: ATOM DENSITIES AND MATERIAL DENSITY

The mixed partial derivative of the leakage with respect to N_1 and ρ , by differentiating Eq. (A.1) with respect to ρ , is

$$\begin{aligned} \frac{\partial^2 L}{\partial \rho \partial N_1} &= q_1 V \frac{\partial P}{\partial \rho} + \frac{\partial Q}{\partial \rho} \sigma_1 \frac{\partial P}{\partial \Sigma} + Q \sigma_1 \frac{\partial}{\partial \rho} \left(\frac{\partial P}{\partial \Sigma} \right) \\ &= q_1 V \frac{\partial P}{\partial \Sigma} \frac{\partial \Sigma}{\partial \rho} + \frac{Q_0}{\rho_0} \sigma_1 \frac{\partial P}{\partial \Sigma} + Q \sigma_1 \frac{\partial}{\partial \Sigma} \left(\frac{\partial P}{\partial \Sigma} \right) \frac{\partial \Sigma}{\partial \rho} \\ &= \left(q_1 V \frac{\Sigma}{\rho} + \frac{Q}{\rho} \sigma_1 \right) \frac{\partial P}{\partial \Sigma} + Q \sigma_1 \frac{\Sigma}{\rho} \frac{\partial^2 P}{\partial \Sigma^2}. \end{aligned} \quad (\text{A.28})$$

The mixed partial derivative of the leakage with respect to N_2 and ρ , by differentiating Eq. (A.2) with respect to ρ , is

$$\begin{aligned} \frac{\partial^2 L}{\partial \rho \partial N_2} &= \frac{\partial Q}{\partial \rho} \sigma_2 \frac{\partial P}{\partial \Sigma} + Q \sigma_2 \frac{\partial}{\partial \rho} \left(\frac{\partial P}{\partial \Sigma} \right) \\ &= \frac{Q_0}{\rho_0} \sigma_2 \frac{\partial P}{\partial \Sigma} + Q \sigma_2 \frac{\partial}{\partial \Sigma} \left(\frac{\partial P}{\partial \Sigma} \right) \frac{\partial \Sigma}{\partial \rho} \\ &= \frac{Q}{\rho} \sigma_2 \frac{\partial P}{\partial \Sigma} + Q \sigma_2 \frac{\Sigma}{\rho} \frac{\partial^2 P}{\partial \Sigma^2}. \end{aligned} \quad (\text{A.29})$$

Differentiating Eq. (A.16) or (A.17) with respect to N_1 and (separately) N_2 also yields Eqs. (A.28) and (A.29).

Another way to do this that recognizes that atom densities and material density are not independent is to apply the chain rule:

$$\frac{\partial^2 L}{\partial \rho \partial \alpha} = \sum_{i=1}^2 \frac{\partial}{\partial N_i} \left(\frac{\partial L}{\partial \alpha} \right) \frac{\partial N_i}{\partial \rho}. \quad (\text{A.30})$$

The atom density of Eq. (103) can be written as

$$N_i = \frac{\rho N_{i,0}}{\rho_0}, \quad i = 1, 2. \quad (\text{A.31})$$

Using Eq. (A.31) and $\alpha = N_1$ yields

$$\begin{aligned} \frac{\partial^2 L}{\partial \rho \partial N_1} &= \frac{\partial^2 L}{\partial N_1^2} \frac{\partial N_1}{\partial \rho} + \frac{\partial^2 L}{\partial N_1 \partial N_2} \frac{\partial N_2}{\partial \rho} \\ &= \frac{N_{1,0}}{\rho_0} \frac{\partial^2 L}{\partial N_1^2} + \frac{N_{2,0}}{\rho_0} \frac{\partial^2 L}{\partial N_1 \partial N_2}. \end{aligned} \quad (\text{A.32})$$

Using Eq. (A.31) and $\alpha = N_2$ yields

$$\begin{aligned} \frac{\partial^2 L}{\partial \rho \partial N_2} &= \frac{\partial^2 L}{\partial N_1 \partial N_2} \frac{\partial N_1}{\partial \rho} + \frac{\partial^2 L}{\partial N_2^2} \frac{\partial N_2}{\partial \rho} \\ &= \frac{N_{1,0}}{\rho_0} \frac{\partial^2 L}{\partial N_1 \partial N_2} + \frac{N_{2,0}}{\rho_0} \frac{\partial^2 L}{\partial N_2^2}. \end{aligned} \quad (\text{A.33})$$

Rearranging Eq. (A.31) and using Eqs. (A.3) through (A.5), it can be shown that Eqs. (A.32) and (A.33) are equal to Eqs. (A.28) and (A.29), respectively.

These density derivatives are constant-volume partial derivatives.⁹

A.IX. MIXED DERIVATIVES: CROSS SECTIONS AND MATERIAL DENSITY

Using Eq. (A.31), the mixed partial derivative of the leakage with respect to σ_1 and ρ , by differentiating Eq. (A.6) with respect to ρ , is

$$\begin{aligned} \frac{\partial^2 L}{\partial \rho \partial \sigma_1} &= \frac{\partial Q}{\partial \rho} N_1 \frac{\partial P}{\partial \Sigma} + Q \frac{\partial N_1}{\partial \rho} \frac{\partial P}{\partial \Sigma} + Q N_1 \frac{\partial}{\partial \rho} \left(\frac{\partial P}{\partial \Sigma} \right) \\ &= \frac{Q_0}{\rho_0} N_1 \frac{\partial P}{\partial \Sigma} + Q \frac{N_{1,0}}{\rho_0} \frac{\partial P}{\partial \Sigma} + Q N_1 \frac{\partial}{\partial \Sigma} \left(\frac{\partial P}{\partial \Sigma} \right) \frac{\partial \Sigma}{\partial \rho} \\ &= \frac{Q N_1}{\rho} \left(2 \frac{\partial P}{\partial \Sigma} + \Sigma \frac{\partial^2 P}{\partial \Sigma^2} \right). \end{aligned} \quad (\text{A.34})$$

The mixed partial derivative of the leakage with respect to σ_2 and ρ , by differentiating Eq. (A.7) with respect to ρ , is

$$\begin{aligned}
\frac{\partial^2 L}{\partial \rho \partial \sigma_2} &= \frac{\partial Q}{\partial \rho} N_2 \frac{\partial P}{\partial \Sigma} + Q \frac{\partial N_2}{\partial \rho} \frac{\partial P}{\partial \Sigma} + Q N_2 \frac{\partial}{\partial \rho} \left(\frac{\partial P}{\partial \Sigma} \right) \\
&= \frac{Q_0}{\rho_0} N_2 \frac{\partial P}{\partial \Sigma} + Q \frac{N_{2,0}}{\rho_0} \frac{\partial P}{\partial \Sigma} + Q N_2 \frac{\partial}{\partial \Sigma} \left(\frac{\partial P}{\partial \Sigma} \right) \frac{\partial \Sigma}{\partial \rho} \\
&= \frac{Q N_2}{\rho} \left(2 \frac{\partial P}{\partial \Sigma} + \Sigma \frac{\partial^2 P}{\partial \Sigma^2} \right). \quad (\text{A.35})
\end{aligned}$$

Differentiating Eq. (A.16) or Eq. (A.17) with respect to σ_1 and (separately) σ_2 also yields Eqs. (A.34) and (A.35).

These density derivatives are constant-volume partial derivatives.⁹

A.X. MIXED DERIVATIVES: SOURCE EMISSION RATES AND MATERIAL DENSITY

Using Eq. (A.31), the mixed partial derivative of the leakage with respect to q_1 and ρ , by differentiating Eq. (A.11) with respect to ρ , is

$$\begin{aligned}
\frac{\partial^2 L}{\partial \rho \partial q_1} &= \frac{\partial N_1}{\partial \rho} V P + N_1 V \frac{\partial P}{\partial \rho} \\
&= \frac{N_{1,0}}{\rho_0} V P + N_1 V \frac{\partial P}{\partial \Sigma} \frac{\partial \Sigma}{\partial \rho} \\
&= \frac{N_1 V}{\rho} \left(P + \Sigma \frac{\partial P}{\partial \Sigma} \right). \quad (\text{A.36})
\end{aligned}$$

The mixed partial derivative of the leakage with respect to q_2 and ρ is zero. Differentiating Eq. (A.16) or Eq. (A.17) with respect to q_1 also yields Eq. (A.36).

These density derivatives are constant-volume partial derivatives.⁹

Acknowledgments

This work was funded by the U.S. National Nuclear Security Administration's Office of Defense Nuclear Nonproliferation Research & Development.

ORCID

Dan G. Cacuci  <http://orcid.org/0000-0001-5417-5701>

References

1. D. G. CACUCI, "Second-Order Adjoint Sensitivity Analysis Methodology (2nd-ASAM) for Computing Exactly and Efficiently First- and Second-Order Sensitivities in Large-Scale Linear Systems: I. Computational Methodology," *J. Comp. Phys.*, **284**, 687 (2015); <https://doi.org/10.1016/j.jcp.2014.12.042>.
2. D. G. CACUCI, "Second-Order Adjoint Sensitivity Analysis Methodology (2nd-ASAM) for Computing Exactly and Efficiently First- and Second-Order Sensitivities in Large-Scale Linear Systems: II. Illustrative Application to a Paradigm Particle Diffusion Problem," *J. Comp. Phys.*, **284**, 700 (2015); <https://doi.org/10.1016/j.jcp.2014.11.030>.
3. D. G. CACUCI, *Sensitivity and Uncertainty Analysis, Volume I: Theory*, Chap. II, Chapman & Hall/CRC, New York (2003).
4. D. G. CACUCI, "Sensitivity Theory for Nonlinear Systems: I. Nonlinear Functional Analysis Approach," *J. Math. Phys.*, **22**, 2794 (1981); <https://doi.org/10.1063/1.525186>.
5. D. G. CACUCI, "Sensitivity Theory for Nonlinear Systems: II. Extensions to Additional Classes of Responses," *J. Math. Phys.*, **22**, 2803 (1981); <https://doi.org/10.1063/1.524870>.
6. K. M. CASE, F. DE HOFFMANN, and G. PLACZEK, "Introduction to the Theory of Neutron Diffusion," Vol. 1, Los Alamos Scientific Laboratory, United States Atomic Energy Commission (1953).
7. P. HUMBERT, "Application of Inverse Gamma Transport to Material Thickness Identification with SGRD Code," *Proc. 13th Int. Conf. Radiation Shielding (ICRS-13) & 19th Topl. Mtg. Radiation Protection and Shielding Division of the American Nuclear Society (RPSD-2016)*, Paris, France, October 3–6 (2016); *European Physics Journal—Web of Conferences*, **153**, 06011 (2017); <https://doi.org/10.1051/epjconf/201715306011>.
8. R. E. ALCOUFFE et al., "PARTISN: A Time-Dependent, Parallel Neutral Particle Transport Code System, Version 7.72," LA-UR-08-7258, Los Alamos National Laboratory (Mar. 2015).
9. J. A. FAVORITE, "Adjoint-Based Constant-Mass Partial Derivatives," *Ann. Nucl. Energy*, **110**, 1052 (2017); <https://doi.org/10.1016/j.anucene.2017.08.015>.
10. J. J. DUDERSTADT and W. R. MARTIN, *Transport Theory*, Chap. 2.1.6, John Wiley & Sons, New York (1979).
11. R. GUNNICK, J. E. EVANS, and A. L. PRINDLE, "A Reevaluation of the Gamma-Ray Energies and Absolute Branching Intensities of ^{237}U , $^{238,239,240,241}\text{Pu}$, and ^{241}Am ," UCRL-52139, Lawrence Livermore National Laboratory (Oct. 1976).
12. J. A. FAVORITE, "Second-Order Reactivity Worth Estimates Using an Off-the-Shelf Multigroup Discrete Ordinates Transport Code," *Proc. Int. Conf. Physics of Reactors (PHYSOR'08)*, Interlaken, Switzerland, September 14–19, 2008 (CD-ROM).

13. J. R. KNOWLES et al., “Determining Physical Parameters of Shielded Uranium Using Gamma Spectroscopy and the Differential Evolution Adaptive Metropolis (DREAM) Method,” *Trans. Am. Nucl. Soc.*, **116**, 559 (2017).
14. R. GUNNICK and J. F. TINNEY, “Analysis of Fuel Rods by Gamma-Ray Spectroscopy,” UCRL-51086, Appendix C, Lawrence Livermore National Laboratory (Aug. 1971).
15. J. MATTINGLY, “Polyethylene-Reflected Plutonium Metal Sphere: Subcritical Neutron and Gamma Measurements,” SAND2009-5804 Rev. 3, Sandia National Laboratories (July 2012).
16. E. C. MILLER et al., “Computational Evaluation of Neutron Multiplicity Measurements of Polyethylene-Reflected Plutonium Metal,” *Nucl. Sci. Eng.*, **176**, 167 (2014); <https://doi.org/10.13182/NSE12-53>.